JCI The Journal of Clinical Investigation

Surface receptor Toso controls B cell–mediated regulation of T cell immunity

Jinbo Yu, … , Niko Föger, Kyeong-Hee Lee

J Clin Invest. 2018. https://doi.org/10.1172/JCI97280.

Research Article In-Press Preview **Immunology** **Inflammation**

The immune system is tightly controlled by regulatory processes that allow for the elimination of invading pathogens, while limiting immunopathological damage to the host. In the present study, we found that conditional deletion of the cell surface receptor Toso on B cells unexpectedly resulted in impaired proinflammatory T cell responses, which led to impaired immune protection in an acute viral infection model, while, in a chronic inflammatory context, was associated with reduced immunopathological tissue damage. Toso exhibited its B cell-inherent immunoregulatory function by negatively controlling the pool of IL-10-competent B1 and B2 B cells, which were characterized by a high degree of self-reactivity and were shown to mediate immunosuppressive activity on inflammatory T cell responses in vivo. Our results indicate that Toso is involved in the differentiation/maintenance of regulatory B cells by fine-tuning B cell receptor (BCR)-activation thresholds. Furthermore, we showed that during influenza A-induced pulmonary inflammation the application of Toso-specific antibodies selectively induced IL-10-competent B cells at the site of inflammation and resulted in decreased proinflammatory cytokine production by lung T cells. These findings suggest that Toso may serve as a novel therapeutic target to dampen pathogenic T cell responses via the modulation of IL-10-competent regulatory B cells.

Title: Surface receptor Toso controls B cell-mediated regulation of T cell immunity

Authors: Jinbo Yu[1,2,5], Vu Huy Hoang Duong[1,2,5], Katrin Westphal[1,2], Andreas Westphal[1,2], Abdulhadi Suwandi[3], Guntram A. Grassl[3], Korbinian Brand[2], Andrew C. Chan[4], Niko Föger[1,2,6] and Kyeong-Hee Lee[1,2,6]

Affiliations:

[1]Inflammation Research Group, [2]Institute of Clinical Chemistry, Hannover Medical School, 30625 Hannover, Germany

[3]Institute of Medical Microbiology and Hospital Epidemiology and German Center for Infection Research (DZIF), Partner Site Hannover, Hannover Medical School, Carl-Neuberg-Str. 1, 30625 Hannover, Germany

[4]Research, Genentech, 1 DNA Way, South San Francisco, CA 94080, USA

[5]J.Y. and V.H.H.D. contributed equally to this work

[6]N.F. and K.-H.L. shared senior authorship

Correspondence should be addressed to:

Prof. Dr. Kyeong-Hee Lee
Institute of Clinical Chemistry and Inflammation Research
Hannover Medical School
Carl-Neuberg-Str. 1
D-30625 Hannover
Tel.: +49 511 532 5285; Fax: +49 511 532 8523
E-mail: Lee.Kyeong-Hee@mh-hannover.de

Conflict of interest statement:

The authors have declared that no conflict of interest exists.

Abstract

The immune system is tightly controlled by regulatory processes that allow for the elimination of invading pathogens, while limiting immunopathological damage to the host. In the present study, we found that conditional deletion of the cell surface receptor Toso on B cells unexpectedly resulted in impaired proinflammatory T cell responses, which led to impaired immune protection in an acute viral infection model, while, in a chronic inflammatory context, was associated with reduced immunopathological tissue damage. Toso exhibited its B cell-inherent immunoregulatory function by negatively controlling the pool of IL-10-competent B1 and B2 B cells, which were characterized by a high degree of self-reactivity and were shown to mediate immunosuppressive activity on inflammatory T cell responses *in vivo*. Our results indicate that Toso is involved in the differentiation/maintenance of regulatory B cells by fine-tuning B cell receptor (BCR)-activation thresholds. Furthermore, we showed that during influenza A-induced pulmonary inflammation the application of Toso-specific antibodies selectively induced IL-10-competent B cells at the site of inflammation and resulted in decreased proinflammatory cytokine production by lung T cells. These findings suggest that Toso may serve as a novel therapeutic target to dampen pathogenic T cell responses via the modulation of IL-10-competent regulatory B cells.

Introduction

A key feature of the immune system is to maintain a delicate balance that provides protection against infectious agents, while minimizing immune-mediated tissue damage. To achieve this critical equilibrium, tight regulatory mechanisms have evolved to control protective immune responses and to avoid misguided or excessive inflammation. It is now well established, that a subset of $CD4^+$ T cells, termed regulatory T cells, exhibit immunosuppressive function and are crucial for the maintenance of normal immune homeostasis by controlling inflammation and preventing autoimmunity (1). More recently, it has been recognized that B cells can also negatively regulate T cell responses in an antibody independent manner. A suppressive role of B cells in pathogenic T cell responses was already suggested in 1996 by Janeway and colleagues, who showed that B cell deficient mice exhibited exacerbated disease in experimental autoimmune encephalomyelitis (EAE) (2). An increasing number of reports has since indicated immunoregulatory function of B cells in various disease models, including T cell-dependent autoimmune models (3-8), transplantation (9), inflammation (10) and cancer (11), which has led to the concept of regulatory B cells (Bregs). Bregs exhibit their regulatory function primarily via the release of IL-10, although other mechanisms may also be involved (12). *In vivo* identification of Bregs is complicated by the description of multiple different Breg subsets with partially overlapping phenotypes and surface marker characteristics in different mouse and human model systems (13). Until now, no Breg-defining transcription factor or unique lineage marker has been identified and Bregs are mainly defined by their ability to secrete IL-10. The nature and origin of Bregs cells is still controversial and it is unclear whether they represent a distinct B cell lineage or a dynamic cellular state.

Toso, also known as Faim3 (Fas apoptosis inhibitory molecule 3) or FcμR (Fc Receptor for IgM), is a type I transmembrane protein belonging to the immunoglobulin gene superfamily. Expression of Toso is restricted to lymphoid organs, where it is particularly highly expressed in B cells. In humans, a tight association of Toso overexpression with B cell malignancy has been observed in patients with chronic lymphocytic leukemia (CLL) (14-16). Toso was originally identified as a surface molecule with negative regulatory function on lymphocyte apoptosis (17, 18). Subsequently, additional studies have identified Toso as an Fc-receptor for soluble IgM (Fcμ-receptor) (19, 20). More recently, it has been demonstrated that Toso physically interacts with membrane IgM-containing B cell antigen-receptor (BCR)-complexes on the surface of mature B

cells and/or within the trans-Golgi-network of developing B cells (21, 22). Functionally, increasing evidence suggests that Toso serves as a physiologically important immunoregulatory molecule for B and T cells. Toso-deficient mice have been reported to show enhanced serum levels of IgM and IgG autoantibodies (21, 23-25), which, however, are not associated with autoimmune pathology (26). Furthermore, studies on Toso-deficient mice have revealed strong immunoprotective function of Toso in a model of *Listeria* infection (27) and during lymphocytic choriomeningitis virus (LCMV) infection (28). Toso deficient mice are also largely resistant to the development EAE and exhibit reduced pathogenic T cell responses (29). The mechanism underlying the phenotypic defects of Toso-deficient mice remains a controversial issue and models involving different effector mechanisms and different immune cell types have been proposed (21, 22, 27, 29). Particularly, it is unclear whether the effects of Toso on tolerance in the B cell compartment are interrelated with impaired immune protection in Toso-deficient mice.

We here demonstrate that the specific deletion of Toso on B cells results in impaired anti-viral T cell responses. We provide evidence that links this immunoregulatory function of B cells on T cell immunity to a specific set of IL-10-competent B cells. Our data show that these regulatory B cells are negatively regulated by Toso and exhibit high prevalence for self-reactivity. Thus, via controlling the pool of regulatory B cells, Toso exhibits a dual role on immune homeostasis; it maintains normal self-tolerance within the B cell compartment and, at the same time, ensures protective T cell immunity against infection.

Results

Toso-deficiency results in increased mortality and reduced production of proinflammatory cytokines by T cells upon influenza infection.

To assess the impact of Toso on immune responses during acute viral infection, we intranasally infected WT and Toso$^{-/-}$ mice with 1000 PFU of influenza virus strain A/PR8 (H1N1). Whereas 84% of WT animals survived infection, Toso$^{-/-}$ mice exhibited significantly increased mortality, with most Toso$^{-/-}$ mice dying between day 10 and 15 post infection (*p.i.*) and only 23% of mice surviving (**Figure 1A**). Pulmonary viral titers in the BAL fluid were comparable between WT and Toso$^{-/-}$ mice at day 4 *p.i.*, indicating normal viral replication and infectivity, but were relatively increased in Toso$^{-/-}$ mice during the clearance phase (day 7 *p.i.*) (**Supplemental Figure 1A**). Thus, increased influenza-induced mortality of Toso$^{-/-}$ mice was associated with delayed viral clearance. Anti-viral immunity and recovery from influenza infection, is largely dependent on effector T cell responses (30, 31), which usually peak around day 9 – 10 *p.i.*, just when Toso$^{-/-}$ mice start to become moribund.

We thus next examined virus-specific T cell responses in Toso$^{-/-}$ mice. Viral antigen-specific CD4$^+$ and CD8$^+$ T cell populations were enumerated in the lung of infected animals at day 9 *p.i.* by tetramer staining for the immunodominant CD4 T cell epitope $NP_{311-324}/IA^b$ (NP311), or the CD8 T cell epitope $NP_{366-374}/D^b$ (NP366). Both, frequency and absolute numbers of virus-specific NP311-tetramer$^+$ CD4$^+$ T cells and NP366-dextramer$^+$ CD8$^+$ T cells were comparable between WT and Toso$^{-/-}$ mice (**Figure 1, B and C**), indicating normal antigen-specific priming and clonal expansion of virus-specific T cells in Toso$^{-/-}$ mice.

Effector T cells contribute to viral control and elimination by the production of potent proinflammatory cytokines such as TNFα and IFNγ. The percentage, as well as absolute numbers of IFNγ- and TNFα-producing T cells from lungs of influenza A infected mice was significantly reduced Toso$^{-/-}$ mice with both CD4+ and CD8+ T cells being affected (**Figure 1, D-G**). Reduced production of these important anti-viral cytokines (IFNγ and TNFα) by Toso$^{-/-}$ T cells was also observed in the spleen of infected animals, irrespective if mice were infected with a high dose (1000 PFU) or low dose (50 PFU) of influenza virus (**Supplemental Figure 1, B-G**, and data not shown), the latter not inducing any mortality in WT or Toso$^{-/-}$ mice.

Thus, although T cells in Toso$^{-/-}$ mice were capable of being activated and to expand in response to viral infection, these T cells were compromised in mounting an efficient anti-viral cytokine response.

Conditional deletion of Toso in B cells results in impaired protective T cell immunity and limits immunopathological tissue damage

To assess whether reduced production of proinflammatory cytokines by T cells in Toso$^{-/-}$ mice is a T cell intrinsic defect that depends on the specific deletion of Toso in T cells, or whether this is an indirect effect mediated via other cell types, such as e.g. antigen-presenting dendritic cells or B cells, we employed a conditional gene targeting approach. To this end, we crossed Toso$^{f/f}$ mice onto different Cre-recombinase expressing transgenic mouse lines – CD4-Cre mice, CD11c-Cre mice and CD19-Cre mice – to specifically delete Toso in T cells, dendritic cells (DCs), and B cells, respectively (**Supplemental Figure 2**).

Upon influenza A infection, virus-induced mortality, as well as IFNγ and TNFα production by T cells was not affected by ablation of Toso in T cells (Toso$^{f/f}$/CD4-Cre$^{+/-}$ mice) (**Figure 2A** and **Supplemental Figure 3, A-D**). Overall survival and T cell responses were also normal in Toso$^{f/f}$/CD11c-Cre$^{+/-}$ mice (**Figure 2B** and **Supplemental Figure 3, E-H**), indicating that conditional deletion of Toso in DCs does not compromise their capacity to efficiently prime T cell activation. To our surprise, increased virus-induced lethality and impaired production of proinflammatory cytokines by T cells was only observed upon specific deletion of Toso in B cells (Toso$^{f/f}$/CD19-Cre$^{+/-}$ mice) (**Figure 2, C-G**). Similar to straight Toso$^{-/-}$ mice (**Figure 1A**), most Toso$^{f/f}$/CD19-Cre$^{+/-}$ mice died between day 10 – 15 *p.i.* (only 11% survival), whereas 88% of CD19-Cre$^{+/-}$ control mice survived infection (**Figure 2C**). Also, the functional ability of CD4^{+} and CD8^{+} T cells to produce IFNγ and TNFα was significantly impaired in Toso$^{f/f}$/CD19-Cre$^{+/-}$ mice compared to CD19-Cre$^{+/-}$ control mice (**Figure 2, D-G**). These data strongly indicate that the functional defect of T cells in Toso-deficient mice is not a T cell intrinsic phenotype, but rather is indirectly induced by Toso-deficient B cells. Upon influenza infection, Toso$^{f/f}$/CD19-Cre$^{+/-}$ mice also had significantly more CD4^{+} T cells expressing PD-1 (**Figure 2H** and **Supplemental Figure 4A**), an inhibitory surface receptor that has been associated with T cell exhaustion (32). Interestingly, increased PD-1 expression on CD4^{+} T cells upon Toso deletion in

B cells correlated with increased expression of its cognate ligand PD-L2 on $CD19^+$ B cells (**Figure 2I** and **Supplemental Figure 4B**).

We further extended our studies on the B cell-specific role of Toso to a model of infection-induced intestinal pathology, employing infection with attenuated *Salmonella* typhimurium. In this model, chronic *Salmonella* infection of the murine gastrointestinal tract is associated with severe immunopathology that manifests in tissue fibrosis and extensive damage to the gut tissue along with the expression of a characteristic Th1-dominated inflammatory cytokine profile (33). Utilizing this model, conditional deletion of Toso on B cells in $Toso^{f/f}$/CD19-$Cre^{+/-}$ mice led to impaired production of TNFα by $CD4^+$ and $CD8^+$ T cells, which was associated with significantly attenuated overall cecal pathology (mainly attributable to reduced tissue damage in the epithelium and the mucosa) and relative protection from weight loss compared to CD19-$Cre^{+/-}$ control mice (**Supplemental Figure 5**).

Together, our data suggest that while expression of Toso on B cells is associated with enhanced protective T-cell immunity during acute infection, it may also contribute to T cell-mediated immunopathological tissue damage under chronic inflammatory conditions.

Toso-deficiency results in increased numbers of IL-10-producing B cells

The unexpected finding that T cell effector function is indirectly regulated by Toso-expression on B cells, prompted us to analyze functional characteristics of Toso-deficient B cells. Here, we first assessed the capacity of $Toso^{-/-}$ B cells to produce the anti-inflammatory cytokine IL-10. To this end, purified B cells from WT and $Toso^{-/-}$ mice were treated for 24h with BAFF, LPS, anti-CD40 or anti-IgM or were control treated. Most interestingly, $Toso^{-/-}$ B cells exhibited a strongly increased capacity to produce IL-10 when compared to WT B cells (**Figure 3A**). Depending on the stimulus, splenic B cells from $Toso^{-/-}$ mice induced up to 4-fold higher frequency and numbers of IL-10-producing cells (**Figure 3, B and C**). Increased production of IL-10 by B cells from Toso-deficient mice is a B cell intrinsic phenotype, as it was specifically observed upon conditional deletion of Toso in B cells ($Toso^{f/f}$/CD19-$Cre^{+/-}$ mice), whereas B cells from $Toso^{f/f}$/CD4-$Cre^{+/-}$ mice and $Toso^{f/f}$/CD11c-$Cre^{+/-}$ mice exhibited normal IL-10 production (**Figure 3, D and E**). B cell cytokine production was, however, not generally affected by Toso-

deficiency, as activation-induced TNFα-production was normal in Toso$^{-/-}$ B cells (**Supplemental Figure 6**).

While only small numbers of IL-10-competent B cells are found in naïve mice, number and frequency of IL-10-producing cells expand considerably upon influenza A infection (**Figure 3, F and G**). Importantly, also under these conditions of an *in vivo* viral infection, splenic B cells from Toso$^{-/-}$ mice had a significantly higher capacity to produce IL-10, as compared to B cells from WT mice (**Figure 3, F and G**). Total B cell counts in the spleen and numbers of GL7^{+}CD95^{+} germinal center B cells were similar between WT and Toso$^{-/-}$ mice upon influenza A infection (**Supplemental Figure 7**). Finally, upon acute infection with influenza A virus, significantly higher frequency and numbers of IL-10-competent B cells were detected in the lungs of Toso$^{f/f}$/CD19-Cre$^{+/-}$ mice compared to CD19-Cre$^{+/-}$ control mice (**Figure 3H**). Thus, taken together, our data suggests that Toso expression on B cells exhibits a B cell intrinsic negative regulatory function on the capacity of these cells to produce the anti-inflammatory cytokine IL-10 both, under steady-state conditions and in an inflammatory setting during viral infection.

Phenotypic characteristics of IL-10-competent B cell subsets

We next extended our analysis of IL-10-producing B cells onto different B cell subsets. Flow cytometric analysis of B cells from Vert-X IL-10 reporter mice – an IL-10-IRES-GFP knock-in mouse strain – showed that upon LPS-induction essentially all splenic B1 cells (CD19^{+}B220^{lo}), as well as a small, but significant fraction of B2 cells (CD19^{+}B220^{hi}) produced IL-10, as indicated by GFP expression (**Supplemental Figure 8A**). Thus, IL-10-competent B cells subsets reside within both, B1 and B2 B cell compartments. IL-10-producing B1 cells exhibited a CD5^{hi} phenotype and showed low expression for CD1d, while, in line with previous reports (34), IL-10-producing B2 B cells were mainly characterized as CD1d^{hi}CD5^{int} cells. Importantly, intracellular IL-10 staining of activated WT and Toso$^{-/-}$ B cells revealed that both of these IL-10 producing B cell populations – IL-10-producing B1a cells (B220^{lo}), as well as IL-10-producing B2 cells (B220^{hi}) – were markedly increased in B cell cultures from Toso$^{-/-}$ mice, irrespective if IL-10 production was induced by treatment with BAFF/IL-21, LPS or CpG-oligodenucleotides (**Figure 4, A-C**).

Based on B220 surface staining and the characteristic expression of CD1d on IL-10-producing B2 B cells, we were able to efficiently identify IL-10-competent B1 and B2 B cell subsets within untreated naïve $CD19^+$ B cells. High purity cell sorting experiments showed that more than 90% of naïve sorted $B220^{lo}$ B1 cells could be induced to produce IL-10 (**Figure 4, D and E**). IL-10-competent B cells were also highly enriched within naïve $B220^{hi}CD1d^+$ B2 B cells, where ~50% of sorted cells could be induced to express IL-10 (**Fig. 4E**). In contrast, the large population of $B220^{hi}CD1d^-$ B2 B cells was largely unable to produce IL-10. We also examined whether IL-10-competent $B220^{hi}CD1d^+$ B2 cells are interrelated with $B220^{hi}AA4.1^+$ transitional B2 cells, however these two B2 B cell subsets were clearly distinct by CD1d vs AA4.1 surface expression (**Figure 4F**) and, importantly, IL-10 production could not be induced in $B220^{hi}AA4.1^+$ transitional B cells (**Figure 4G**), thus also functionally confirming the different nature of these two different B cell subsets. Marginal zone precursor (MZP) B cells, which have been implicated in IL-10 production in a model of experimental arthritis (4), were also largely unable to produce IL-10 in our system (**Supplemental Figure 8, B-E**).

Further phenotypical analysis showed that the $B220^{lo}$ B1 B cell population expresses high levels of CD5 and CD43, typical for B1a B cells, while IL-10-competent $B220^{hi}CD1d^+$ B2 cells exhibit a $CD5^{int}IgM^{hi}IgD^{lo}CD21^{hi}CD23^{lo}$ phenotype reminiscent of marginal zone B cells (**Fig. 4H and Supplemental Figure 8F**). IL-10-incompetent $B220^{hi}CD1d^-$ cells were mainly $IgM^{lo}IgD^{hi}CD21^{int}CD23^{hi}$ follicular B cells (**Fig. 4H**).

Detection of IL-10-producing B cells from influenza-infected mice required short term *ex vivo* restimulation. Here, we observed that IL-10-producing B1 and B2 B cell subsets are substantially expanded in both, lung and spleen from influenza A-infected mice compared to uninfected control mice (**Supplemental Figure 9, A-C)**. Moreover, IL-10-producing B2 B cells (B2/IL-10 cells) from infected mice were also characterized by high expression of CD1d and, under such an inflammatory context, IL-10-producing B1 and B2 B cells showed strong expression of Tim-1, CD73 and FasL (**Supplemental Figure 9, D and E**).

Most importantly, in $Toso^{-/-}$ mice both of the IL-10-competent B cell subsets ($B200^{hi}CD1d^+$ B2 cells and $B220^{lo}$ B1a cells) were significantly increased in frequency and numbers (**Figure 4I**). Interestingly, however, on a per cell basis, the cell intrinsic capacity to produce IL-10 was comparable between the respective B cell subsets from WT and $Toso^{-/-}$ mice (**Fig. 4E**). Thus,

Toso$^{-/-}$ IL-10-competent B cells appeared to be functionally normal, but were present in significantly higher quantities upon genetic ablation of Toso.

Suppressive function of IL-10-producing regulatory B cells

IL-10-producing B cells have been described as regulatory B cells that exhibit immune regulatory functions and can downmodulate T cell responses and inflammatory reactions (35, 36). Thus, to demonstrate immunosuppressive activity of IL-10-producing B1 and B2 B cell subsets we performed *in vitro* T cell–B cell co-culture experiments. To this end, B cells from Vert-X IL-10/GFP reporter mice were purified by fluorescence activated cell sorting into IL-10-producing B1 B cells (B220^{lo}GFP^{+}; 'B1/IL-10 cells') and B2 B cells (B220^{hi}GFP^{+}; 'B2/IL-10 cells'), as well as GFP-negative control B cells (B220^{hi}GFP^{-}; B2/effector cells). Sorted B cell populations were added to cultures containing purified naïve CD4^{+} or CD8^{+} T cells. Cultures were stimulated with anti-CD3 mAbs and proinflammatory cytokine production by CD4^{+} and CD8^{+} T cells was assessed. The frequency of IFNγ^{+} and TNFα^{+} CD8^{+} T cells was significantly reduced in co-cultures with B1/IL-10 cells and B2/IL-10 cells, compared to cultures with B2/effector control cells (**Figure 5, A and B**). A similar suppressive effect of IL-10-producing B1 and B2 B cell subsets was observed in co-cultures with naïve CD4^{+} T cells (**Figure 5C**).

Next, we assessed whether freshly isolated naïve B220^{lo} B1a cells and B220^{hi}CD1d^{+} B2 cells can also exhibit immunosuppressive function on T cell immunity. For these experiments on non-activated B cell subsets we performed adoptive transfer of purified naïve B cell subsets followed by *in vivo* viral challenge. 1x10^{6} FACS-sorted CD19^{+}B220^{lo} B1a cells, CD19^{+}B220^{hi}CD1d^{+} B2 B cells, and CD19^{+}B220^{hi}CD1d^{-} B2 B cells from untreated Toso$^{-/-}$ mice were adoptively transferred into C57BL/6 recipient mice. One day after adoptive transfer, mice were intranasally infected with influenza A and cytokine responses in lung T cells were analyzed on day 9 *p.i.* (**Figure 5D**). In animals that had received CD19^{+}B220^{hi}CD1d^{-} cells, virus-induced TNFα- or IFNγ-production by CD4^{+} and CD8^{+} T cells was comparable to normal control animals that had not received any transferred cells (='no transfer') (**Figure 5, E-H**). Adoptive transfer of naïve CD19^{+}B220^{lo} B1a cells, however, had clear suppressive effects on virus-induced cytokine production by CD4^{+} and CD8^{+} T cells (**Figure 5, E-H**). Reduced TNFα- and IFNγ-production by T cells was also observed upon transfer of naïve CD19^{+}B220^{hi}CD1d^{+} B2 B cells, although its effects were less

pronounced than $CD19^{+}B220^{lo}$ B1a cells, consistent with the greater enrichment of 'IL-10 competency" of $CD19^{+}B220^{lo}$ B1a cells (**Figure 4E**). Based on their immunoregulatory function $CD19^{+}B220^{lo}$ B1a cells are here termed as 'B1-Bregs' and $CD19^{+}B220^{hi}CD1d^{+}$ B2 cells as 'B2-Bregs'. Adoptively transferred naïve B1- and B2-'Bregs' isolated from IL-$10^{-/-}$ mice did not exhibit measurable suppressive activity on proinflammatory cytokine production by $CD4^{+}$ and $CD8^{+}$ T cells during influenza A infection (**Supplemental Figure 10**), suggesting that IL-10 is a critical effector molecule of regulatory B cells *in vivo*, although the involvement of alternative effector mechanisms, such e.g. CD73-mediated adenosine generation, which has been reported to be affected in IL-10-deficient B cells (37), cannot be fully ruled out.

Taken together, adoptive transfer of as little as $1x10^{6}$ cells demonstrates that naïve B1-Bregs and B2-Bregs can both act as physiological regulators of T cell function by suppressing virus-induced T cell cytokine production during acute influenza A infection. Moreover, these data also provide a mechanistic explanation for the impaired T cell responses in Toso$^{-/-}$ mice during influenza A infection, which are likely caused by the higher numbers of immunosuppressive B1 and B2 regulatory B cell subsets in these mice.

B cell development in Toso-deficient mice

Toso surface expression is not restricted to B1 and B2 immunoregulatory B cells, but Toso is rather expressed on all peripheral B cells, with relatively highest expression on $B220^{hi}CD1d^{-}$ effector (follicular) B cells (**Supplemental Figure 11A**). Thus, how Toso specifically affects the generation of regulatory B cell subsets is still puzzling. Consistent with previous reports (24, 25) and the absence of Toso surface expression on early developmental B cell stages, we observed normal development of B cells in the bone marrow (BM) of Toso$^{-/-}$ mice (**Supplemental Figure 11, B-G**). Analysis of splenic B cells from Toso$^{-/-}$ mice revealed reduced frequency of mature $IgM^{lo}IgD^{hi}$ B cells, while the population of $IgM^{hi}IgD^{hi}$ transitional B cells was significantly increased (**Supplemental Figure 12, A and B**). This was further accompanied by an increase in $CD21^{hi}CD23^{lo}$ marginal zone B cells (**Supplemental Figure 12, C and D**), suggesting enhanced differentiation towards this particular B cell subset, which is also consistent with increased numbers of MZ-like B2-Bregs in Toso$^{-/-}$ mice.

In addition to slightly increased surface expression of IgM, we also noted that overall CD21 and CD23 expression levels, as well as CD62L surface levels were slightly downregulated in Toso$^{-/-}$ B cells, further indicating alterations in peripheral B cell maturation/differentiation (**Supplemental Figure 12, E-H**). Expression of CD19, B220, IgD, MHCII, and CD44 was not affected by Toso deficiency (**Supplemental Figure 12H**).

Furthermore, higher numbers of B220^{lo} B1a cells were not only found in the spleen of Toso$^{-/-}$ mice (**Fig. 4I** and **Supplemental Figure 13, A and B**), but also in the peritoneal cavity, where an increase in B1a cells was accompanied by a corresponding decrease in B1b cells (**Supplemental Figure 13, C and D**). Analysis of peritoneal B cells revealed that B1a cells have an extremely high capacity to produce IL-10, whereas B1b cells are substantially less potent in IL-10 production (**Supplemental Figure 13E and F**). Together, Toso appears to be dispensable for B cell development in the BM, but fine tunes maturation/differentiation of specific B cell subsets in the periphery.

Self-reactivity of regulatory B cell subsets

Development of peripheral B cell compartments is tightly regulated and even small changes in B cell maturation/differentiation may alter the balance of peripheral B cell tolerance. We thus next examined serum antibody levels and autoantibody production in Toso$^{-/-}$ mice. Basal levels of serum IgM and IgG were comparable between 8-10 months old WT and Toso$^{-/-}$ mice (**Figure 6A**). However, consistent with published reports (21, 23-25), we detected elevated serum titers of autoreactive antibodies in Toso$^{-/-}$ mice. IgM and IgG antibodies directed against dsDNA or ssDNA were significantly increased in sera from aged Toso$^{-/-}$ mice compared to WT controls (**Figure 6, B and C**), supporting a role of Toso in the maintenance of self-tolerance.

To elucidate the major source of self-reactive antibodies in Toso$^{-/-}$ mice, we analyzed the capacity of different B cell subsets to produce autoantibodies. High purity sorted B1- and B2-Bregs from Toso$^{-/-}$ mice exhibited strong production of anti-dsDNA and anti-ssDNA antibodies upon *in vitro* cultivation with LPS, while, in marked contrast, B2-effector cells and AA4.1^{+} transitional B2 B cells were largely unable to produce self-reactive antibodies (**Figure 6D**). Efficient production of autoantibodies was not a specific feature of Toso$^{-/-}$ Bregs, but was similarly observed in WT B1- and B2-Bregs (**Supplemental Figure 14A**). B2-effector cells and AA4.1^{+} transitional B2 B cells

exhibited only minimal autoantibody production under these conditions, even though they showed efficient blast formation and expression of the plasma cell marker CD138 (**Supplemental Figure 14B**). Together, these data indicate that self-reactive B cells are highly prevalent among B1-Bregs and B2-Bregs. Interestingly, IL-10-competent immunoregulatory B cell numbers rise as mice age and increased numbers of Bregs in Toso$^{-/-}$ versus WT mice become even more pronounced in older mice (**Figure 6, E and F**). It is thus likely that the higher numbers of regulatory B cells in Toso$^{-/-}$ mice are responsible for increased autoantibody levels in Toso$^{-/-}$ mice.

Toso fine-tunes BCR-responsiveness

Regulation of BCR-signaling is a critical determinant for peripheral B cell differentiation/ maintenance and the establishment of tolerance (38-41). We thus next evaluated the effects of Toso-deficiency on BCR-responsiveness and B cell activation/survival. Reflecting their different maturation/differentiation state, overall responsiveness to IgM receptor triggering varied considerably among different CD19^{+} B cell subtypes. Upon anti-IgM stimulation B2-effector cells (B220^{hi}AA4.1^{-}CD1d^{-}) proliferated vigorously, while B2-Bregs (B220^{hi}CD1d^{+}) and the IL-10-incompetent population of transitional B2 cells (B220^{hi}AA4.1^{+}), which both express high levels of IgM, rather showed induction of cell death. B1a B cells (B220^{low}AA4.1^{-}CD1d^{-}; B1-Bregs) were largely unresponsive to anti-IgM triggering (**Figure 6G** and **Supplemental Figure 15, A-E**).

Toso$^{-/-}$ B2-effector cells showed a dose-dependent reduction in anti-IgM-induced cell proliferation, which was primarily associated with reduced cellular survival, while, similar to previous reports (25), the actual rate of cell divisions of live cells was comparable between WT and Toso$^{-/-}$ cells (**Figure 6, H-I**). Toso-deficiency had, however, no effects on anti-IgM-induced survival/apoptosis of B1-Bregs, B2-Bregs or B2-transitional cells (**Supplemental Figure 15, A and B**) and Toso$^{-/-}$ B cells also showed normal survival upon treatment with other stimuli, such as LPS or BAFF + IL-21 (**Supplemental Figure 15, F and G**).

As Toso interacts with the membrane BCR complex (22) and given the effects of Toso-deficiency on B2-effector cell survival/proliferation, we examined the role of Toso on proximal BCR-mediated signaling events and early markers of B cell activation. Upon stimulation with

anti-IgM, Toso-deficient B2-effector cells exhibited slightly impaired and less sustained phosphorylation of the tyrosine kinase Btk, indicating attenuated BCR signaling (**Figure 6J**). Lower Btk-activation correlated with reduced induction of activation markers, such as CD25, CD69 and CD86, in Toso-deficient B cells (**Figure 6, K and L** and **Supplemental Figure 15H**). It is noteworthy that IgM-mediated induction of activation markers was not fully impaired upon Toso deletion, but $Toso^{-/-}$ cells rather exhibited a relative shift in IgM receptor responsiveness (**Figure 6L** and **Supplemental Figure 15H**), indicating altered signaling/activation thresholds. Lower BCR-mediated induction of activation markers was also observed in $Toso^{-/-}$ B2-Bregs and B2-transitional cells, while owing to their cell type intrinsic low BCR responsiveness, B1-Bregs largely failed to respond to anti-IgM stimulation (**Figure 6K**). Together, these data indicate that Toso acts as a signal amplifier to fine-tune BCR-responsiveness.

Anti-Toso treatment modulates IL-10-competent B cell numbers at sites of inflammation and results in impaired T cell responses upon influenza infection

Given the negative regulatory role of Toso on IL-10-competent B cells and their immunosuppressive function on T cell immunity, we sought to investigate the effects of anti-Toso antibody treatment on B and T cell responses in the influenza-induced lung inflammation model and to evaluate its potential for immunomodulatory therapeutic applications. To induce virus-mediated lung inflammation, mice were infected intranasally with influenza A. One day prior to infection and on day 2 and 5 *p.i.* mice were treated with either anti-Toso mAb or control IgG and B cells in inflamed lungs were analyzed on day *9 p.i.*. Noteworthy, Toso is highly expressed on essentially all peripheral B cells, however, *in vivo* anti-Toso mAb application did not result in B cell depletion, as comparable numbers of B cells were detected in lungs of anti-Toso and control IgG treated mice (**Figure 7A**). Treatment with anti-Toso mAb did, however, induce a striking increase in both frequency and absolute numbers of IL-10-competent B cell in lungs from influenza-infected animals (**Figure 7B**). Importantly, consistent with our findings on Toso-deficient mice, increased numbers of IL-10-competent B cells correlated with impaired T cell responses at sites of inflammation, as virus-induced TNFα and IFNγ-production by $CD4^+$ and $CD8^+$ T cells was significantly reduced in lungs of mice that had received Toso mAb compared to control IgG treated mice (**Figure 7, C-F**). Together, these data reemphasize the

immunoregulatory role of Toso during inflammatory disease. Furthermore, as Toso is conserved between mice and humans and is also expressed on human B cells (Ref. 19 and **Supplemental Figure 16**) the data also suggest that Toso may provide a promising therapeutic target to modulate IL-10-competent B cell compartments and to dampen excessive T cell responses at local sites of inflammation.

Discussion

Employing conditional gene deletion, we here demonstrate that impaired anti-viral T cell responses upon influenza A infection in Toso$^{-/-}$ mice, were not due to T cell inherent defects, but rather induced by a previously unrecognized role of Toso in B cells. Our findings thus reveal an unexpected regulatory activity of B cells on T cell function during viral infection. Deletion of Toso on B cells results in a strong increase of IL-10-competent B cells, and, as we further demonstrate, this specific subtype of B cells mediates immunosuppressive activity on T cell responses during viral infection, most likely via an IL-10 dependent mechanism. Immunosuppressive function of IL-10 during influenza infection has been demonstrated in studies on IL-10$^{-/-}$ mice (42, 43). Moreover, B cells have been shown to be a relevant source of IL-10 during viral infection (44). B cells upregulate IL-10 expression during infection with murine cytomegalovirus and this B cell-derived IL-10 decreases virus-specific IFNγ-responses in CD8 T cells (44). Considering our data, we thus propose that Toso promotes efficient anti-viral T cell cytokine responses by restricting the size of the IL-10-competent B cell pool. Specifically, B cell intrinsic expression of Toso restricted differentiation/maintenance of IL-10-competent B cells *in vivo*. At the cellular level, Toso$^{-/-}$ Bregs exhibited normal functions. Hence, the impaired T cell responses observed in Toso$^{-/-}$ mice following influenza infection likely reflect the increased numbers of regulatory B cells in Toso-deficient mice.

The present study demonstrates that IL-10-competent B cells are highly enriched within two distinct subpolulations of B cells, the small fraction of splenic B220^{hi}CD1d^{+}CD5^{int} B2 cells and the fraction of B220^{lo}CD5^{hi} B1a cells. These findings are consistent with earlier descriptions of B1a B cells as highly potent producers of IL-10 (45) and recent reports of an IL-10-competent population of CD19^{hi}CD1d^{+}CD5^{+} B cells, termed B10 cells, that exhibits immunoregulatory function in models of autoimmunity (6, 8, 34, 46). Interestingly, IL-10-competent B220^{hi}CD1d^{+}CD5^{int} B cells share many surface marker characteristics with marginal zone (MZ) B cells.

Adoptive transfer of naïve B cell subsets showed that both major IL-10-competent B cell compartments – B220^{hi}CD1d^{+}CD5^{int} B2 cells (=B2-Bregs) and B220^{lo}CD5^{hi} B1a cells (=B1-Bregs) – exhibit immunosuppressive activity on influenza-induced T cell responses. Adoptively transferred ‘Bregs’ from IL-10-deficient mice did not exhibit such potent suppressive activity on

T cell cytokine production, suggesting that the immunoregulatory function of Bregs is largely mediated via IL-10. It is, however, conceivable that, depending on the specific inflammatory context, additional mechanisms, such as PD-L2/PD-1, CD80/CTLA4, GITR/GITRL or FasL/Fas interactions, secretion of TGFβ or IL-35, or CD73-mediated adenosine generation also contribute to the inhibitory function of B1- and B2-Bregs (37, 47-51).

An important, but largely unexplored aspect of regulatory B cells is their antigen specificity. We here show that IL-10-competent B1- and B2-Bregs exhibit a high prevalence for autoreactivity and readily secrete self-reactive antibodies upon TLR stimulation. Self-reactivity is a typical feature of B1a and MZ B cells, which express polyreactive BCRs that can bind both to pathogens and self-antigens (52). Considering this and the striking similarities in surface marker characteristics between regulatory B cell subsets and B1a / MZ B cells, it is thus an intriguing idea that the majority of regulatory B cells originates from B1a and MZ B cells and/or their precursors – the reported phenotypic diversity of regulatory B cells may be more related to effects of the specific inflammatory milieu and particular tissue environment and/or reflect differences in the cellular activation status. Supporting evidence for this idea comes from earlier studies that have characterized B1 and MZ B cells as major IL-10-producing B cells and have demonstrated regulatory function of these specific B cell subsets in different models of inflammatory disorders and autoimmunity (45, 53-59). Consistent with regulatory B cells being closely related to B1a and MZ B cells, the observed increase in IL-10-competent B cells in Toso$^{-/-}$ mice correlated with a corresponding increase in B1a and MZ B cells. While an increase in B1a cells has also been observed in other Toso-deficient mouse strains, MZ B cell numbers were reported to be either decreased or unchanged (21, 23, 24). Discrepancies in MZ B cell numbers may be due to different targeting strategies and use of different ES cell lines (129/Sv vs B6) and also be related to slightly altered expression levels of CD21 and CD23 in Toso$^{-/-}$ B cells which complicates MZ B cell identification. Given their potential to produce self-reactive antibodies, increased numbers of B1a and MZ B cells likely also account for the elevated, albeit non-pathogenic levels of IgM and IgG autoantibodies that we and others have detected in Toso$^{-/-}$ mice (21, 23-25). In the NZB/W mouse model of systemic lupus erythematosus, B1 and MZ B cells are also expanded and spontaneously secrete IgM autoantibodies and can produce self-reactive, isotype-switched IgG antibodies (60, 61). Consistent with a regulatory capacity of B1a and MZ B

cells, the number of IL-10-producing B cells was also found to be increased in young NZB/W mice prior to disease onset (62).

Together, in analogy to natural regulatory T cells (1), regulatory B cells are characterized by self-reactive antigen receptors and, upon appropriate activation utilize secretion of immunomodulatory cytokines, such as IL-10, as major effector mechanism to prevent excessive inflammatory reactions. Our observation that IL-10-producing B cells expand in numbers and are recruited to the site of inflammation during influenza-induced pulmonary disease thus suggests a scenario in which recognition of self-antigens (which are exposed due to tissue damage) by autoreactive Bregs induces their immunosuppressive activity to dampen the inflammatory response and limit immunopathology. We thus propose, that the population of Bregs is normally tightly controlled, to ensure a well-balanced immune response that allows for efficient immune protection against pathogens while minimizing immunopathological tissue damage. Mice with Toso-deficiency on B cells have increased numbers of Bregs and, thus, a 'dysregulated' system, which results in impaired ('suppressed') proinflammatory T cell responses (see model in **Supplementary Figure 17**). Our data indicate that during acute influenza infection, where anti-viral immune protection is largely dependent on effector T cells, such suppressed T cell responses are detrimental and are associated with impaired immune protection and an increased risk of mortality. In contrast, under chronic inflammatory conditions, such as the chronic bacterial-induced model of colitis, where effector T cells are more associated with immunopathological tissue damage, higher numbers of Bregs and, thus, impaired T cell effector function are beneficial, as this limits T cell-mediated tissue destruction (**Supplementary Figure 17**).

Differentiation and homeostasis of peripheral B cell subsets is critically influenced by signaling through the BCR (38-41). In line with altered peripheral B cell compartments in Toso-deficient mice, we here demonstrate that Toso shifts the threshold for BCR-mediated cellular activation/survival pathways. The exact molecular mechanism of how Toso affects BCR-responsiveness is currently unknown. As an IgM-binding molecule Toso may interact directly with membrane bound IgM containing BCR complexes (22) or, alternatively, may indirectly affect B cell signaling via recognition of soluble IgM immune complexes. Increased tonic signaling in Toso-deficient B cells (21), could not be confirmed in our study and may be related to the unusual occurrence of a lymphoproliferative disorder in this particular strain of mice, which has not been observed in any other strain of Toso-deficient mice.

Infection with influenza virus is frequently associated with severe pulmonary immune pathology in human patients. The anatomical structures in the lung are highly sensitive to tissue destruction, necessitating a fine balance between pro- and anti-inflammatory responses during pulmonary infection. In particular, after viral clearance, excessive release of proinflammatory cytokines by continually recruited CD8 T cells can cause severe lung tissue injury. In the present study, we show that during influenza A-induced pulmonary inflammation the application of Toso blocking antibody selectively induces IL-10-competent B cells at the site of inflammation, an effect that was associated with reduced production of proinflammatory cytokines by lung T cells. These data suggest, that clinical targeting of Toso may provide a novel therapeutic approach to control pathogenic T cell responses via the modulation of IL-10-competent B cell compartments at local sites of inflammation.

Materials and Methods

Mice and viral infection

Constitutive Toso knock-out mice (Toso$^{-/-}$ mice) and the generation of mice with a conditional floxed Toso allele (Toso$^{f/f}$ mice) have been described before (18). In brief, the targeting vector was designed to have exons 4-7 flanked by loxP sites. After transfection into C57BL6 embryonic stem cells targeted ES cell clones were identified by southern blotting and were injected into blastocysts. Upon germline transmission the frt-flanked neomycin-selection cassette was removed by breeding with C57BL/6 flp deleter mice. The resulting floxed-targeted mouse lines were crossed with the EIIa-Cre transgenic mouse (http://www.informatics.jax.org/reference/J:70555) line to obtain Cre-mediated total germline excision of exons 4-7 (constitutive Toso knock-out). Toso-deficient and Toso-floxed mice were backcrossed for >8 generations with C57BL6/J. To obtain cell type specific conditional deletion, Toso-floxed (Toso$^{f/f}$) were crossed with transgenic mouse lines expressing Cre-recombinase under control of the *cd4* promoter (CD4-Cre mice: Tg(Cd4-cre)1Cwi) (http://www.informatics.jax.org/reference/J:73127), the *cd11c (Itgax)* promoter (CD11c-Cre mice: Tg(Itgax-cre,-EGFP)4097Ach) (http://www.informatics.jax.org/reference/J:123556), or the *cd19* promoter (CD19-Cre mice: Cd19$^{tm1(cre)Cgn}$) (http://www.informatics.jax.org/reference/J:67676). Vert-X IL-10 reporter mice (B6(Cg)-Il10$^{tm1.1Karp}$) (http://www.informatics.jax.org/reference/J:151551) that carry an internal ribosome entry site (IRES)-enhanced green fluorescent protein (eGFP) fusion protein downstream of exon 5 of the interleukin 10 (Il10) gene were utilized for some experiments. Cre-expressing transgenic mouse lines, IL-10 reporter mice and IL-10-deficient mice (B6.129P2-Il10^{tm1Cgn}; http://www.informatics.jax.org/allele/MGI:1857199; kindly provided by A. Bleich and I. Brüsch, Hannover Medical School, Hannover, Germany) were all on C57BL/6J background and were originally obtained from The Jackson Laboratory. Mice were housed in individually ventilated cages (IVC) under specific pathogen-free (SPF) conditions in the barrier animal facility at Hannover Medical School. Mice were infected at 10–13 weeks of age. Controls were sex- and age-matched. For *in vivo* influenza infection, mice were anesthetized with ketamine-xylazine. Virus was diluted in sterile PBS and mice were infected by intranasal (*i.n.*) administration of a total volume of 40 µl of PR8 influenza virus. Mice were monitored daily for weight loss, signs of illness and survival. Anti-Toso mAb or control rat IgG (catalog 012-000-003, Jackson

ImmunoResearch) was administered *i.v.* on days -1, 2 and 5 *p.i.* (200 µg/mouse/time point). To examine the primary immune response, cells were harvested from lungs and spleen on the indicated days post infection (*p.i.*). Bronchoalveolar lavage (BAL) fluid was collected for viral titer measurements.

Salmonella infection studies: Streptomycin (20 mg per mouse) was given by oral gavage to mice aged 16 weeks. 24 hours after antibiotic administration, mice were infected with *S.* Typhimurium *ΔaroA* at a dose of 3×10^6 bacteria in 100 µL HEPES buffer (100 mM, pH 8.0). Control mice (mock-infection) were given 100 µL HEPES buffer. For histopathological analysis, tissues were fixed in 10% neutral buffered formalin overnight and embedded in paraffin. Cecum sections (5 µm) were deparaffinized and stained with haematoxylin and eosin (H&E). Histological scores in the ceca of infected mice were determined as previously described (63). Briefly, pathological changes were assessed by evaluating various parameters such as presence of luminal cells, infiltrating immune cells, crypt abscesses and the formation of edema in the respective layer of the intestinal bowel wall including the surface epithelium, mucosa and submucosa.

Influenza virus

Influenza virus strain A/PR8 (A/Puerto Rico/8/34 [H1N1]) was obtained from ATCC. Virus was grown in Madin-Darby canine kidney (MDCK; obtained from ATCC) cells. Viral titers were determined by standard MDCK plaque titration assay. Briefly, serial 10-fold dilutions of virus stock or bronchoalveolar lavage (BAL) fluid from infected mice were allowed to adsorb onto 90% confluent MDCK cells on a 24-well plate. After 2.5 h of incubation cells were overlayed with 1.2% Avicell TC-581 (IMDC) in DMEM (Gibco) supplemented with 0.1 % BSA, 1% L-Glutamine, penicillin, streptomycin and 1 µg/ml TPCK-Trypsin (ThermoFisher) and cultured for 24 h at 37 °C in 5% CO_2. Cells were washed, fixed, permeabilized and virus plaques were visualized and enumerated by staining with a mAb against influenza A nucleoprotein (AA5H, AbD Serotec). Viral titers were calculated as PFU/mL.

Flow cytometry (FACS)

Single-cell suspensions of spleen, bone marrow, and peritoneum were prepared from fresh tissue using standard procedures. To isolate pulmonary lymphocytes, lung lobes were minced and strained through nylon mesh. Following red blood cell lysis, cells were blocked with anti-CD16/32 (clone 93, Biolegend) and subsequently stained with fluorescent-labeled mAbs summarized in supplemental table 1. Anti-Toso mAb (ratIgG2a) directed against the extracellular domain of murine Toso was generated by DNA vaccination and was directly conjugated with DyLight649. APC-labeled MHC-II I-A^b/$NP_{311-325}$ (NP311)-tetramer (containing QVYSLIRPNENPAHK of influenza virus nucleoprotein) was obtained from the NIH Tetramer Core Facility and APC-labeled D^b/$NP_{366-374}$ (NP366)-dextramer (containing ASNENMETM of influenza virus nucleoprotein) was purchased from Immudex. For live/dead cell discrimination, we used the fixable viability dye eFluor450 (eBiosciences). For the detection of intracellular cytokines, cells were restimulated *ex vivo* in the presence of Brefeldin A and Monensin (both eBioscience). After cell surface staining, cells were fixed with paraformaldehyde and permeabilized using Perm/Wash buffer (eBioscience) and stained with following mAbs against TNFα (MP6-XT22), IFNγ (XMG1.2) or IL-10 (JES5-16E3) (all Biolegend). Flow cytometric measurements were performed on a FACSCantoII cell analyzer (BD Biosciences). Data were analyzed with FlowJo software (version 9.9.3, Mac; version 10.0.7, PC; Tree Star).

Cell sorting and adoptive transfer experiments

For high purity cell sorting experiments, splenic B cells were first enriched by magnetic isolation using negative selection (pan-B cell isolation kit; Miltenyi Biotec and Stemcell Technologies). B cell subpopulations were then further purified following immunofluorescence surface staining using high speed flow cytometry cell sorters (FACSAria Fusion and FACSAria IIu, both BD Biosciences). To obtain highly pure B cell subsets with minimal contamination by other cell types, we pre-gated on viable cells that were $CD19^+$, but negative for CD4, CD8, F4/80 and NK1.1. Further gating of B cell subsets was primarily based on B220, CD1d and AA4.1 surface expression or B220 vs. GFP (IL-10) expression. Sorted B cell subsets had >98% purity.

For adoptive transfer experiments, FACS-sorted B cell subsets were immediately transferred *i.v.* into syngeneic C57BL/6J recipient mice ($1x10^6$ cells per recipient mouse). One day after adoptive transfer, mice were infected intranasally (*i.n.*) with influenza virus strain A/PR8. On day

9 post infection, lungs cells were isolated, restimulated *ex vivo* and subjected to flow cytometric analysis.

***Ex vivo* cell restimulation, cell activation and B cell cultures**

For the detection of T cell cytokine production, cells were restimulated *ex vivo* for 5 h in the presence of Brefeldin A and Monensin (both eBioscience) on tissue culture plates that had been pre-coated with anti-CD3 (10µg/ml, clone 145-2C11, eBioscience) and anti-CD28 (2 µg/ml, clone 37.51, Biolegend). Where indicated, splenocytes were restimulated for 6 h with influenza A virus peptide of amino acids 366-374 of the viral nucleoprotein (NP366-peptide), an H-2K^b restricted epitope that is specific for CD8$^+$ T cells, in the presence of Brefeldin A and Monensin. To assess IL-10 production by B cells during influenza A virus infection, cells were restimulated *ex vivo* for 5 h with PMA (50 ng/ml, Sigma) and ionomycin (500 ng/ml, Sigma) in the presence of Brefeldin A and Monensin. Following *ex vivo* restimulation, cells were subjected to cell surface and intracellular FACS staining.

For the *in vitro* analysis of IL-10 production by B cells, isolated leukocytes or purified B cell populations were cultured for the indicated times either with ultrapure LPS (500 ng/ml, InvivoGen), CpG oligonucleaotides (10 µg/ml, InvivoGen), BAFF (200 ng/ml, Biolegend), anti-CD40 (10 µg/ml, clone 1C10, Biolegend), anti-IgM (10 µg/ml, goat-anti-mouse F(ab')$_2$ fragment, Jackson ImmunoResearch) or a combination of BAFF (200 ng/ml) plus IL-21 (50 ng/ml, Biolegend). PMA (50 ng/ml, Sigma) and ionomycin (500 ng/ml, Sigma) plus Brefeldin A and Monensin (both eBioscience) was added during the last 5 h of culture. Cells were subsequently analyzed by intracellular flow cytometry.

For some experiments, FACS-sorted B cell populations were stimulated for the indicated times with titrated amounts of anti-IgM (goat-anti-mouse F(ab')$_2$ fragment, Jackson ImmunoResearch) and cultures were subsequently analyzed by flow cytometry for cell survival and upregulation of activation markers. To analyze *in vitro* autoantibody production, FACS-sorted B cell populations were stimulated for 3 days as indicated. Culture supernatants were then collected for the detection of autoantibodies and cells were analyzed by flow cytometry.

For the analysis of B cell signaling, FACS-sorted B effector cells were stimulated with anti-IgM (10 µg/ml, goat-anti-mouse $F(ab')_2$ fragment, Jackson ImmunoResearch). Stimulation was stopped by fixation in paraformaldehyde. Cells were then permeabilized using Perm/Wash buffer (eBioscience), stained with anti-phospho-Btk/Itk (Tyr551, Tyr511; eBioscience) and analyzed by flow cytometry.

ELISA and detection of autoantibodies

Serum titers of IgM and IgG were determined by specific ELISA kits (eBioscience) according to the manufacturer's protocol. To detect autoantibodies in serum and cell culture supernatants, high binding ELISA plates (Greiner) were coated o/n with 2 µg/ml single (ss)- or double (ds)-stranded DNA from calf thymus (Sigma). ssDNA was obtained by heat denaturation of dsDNA (95 °C, 10 min) followed by rapid cooling on ice. Coated plates were blocked with 1% BSA, 0.5% gelatin in TBS for 2h at RT and diluted samples were incubated o/n at 4 °C in TBS 1% BSA. Bound anti-ssDNA or anti-dsDNA Abs were detected with HRP-conjugated anti-mouse IgG (eBioscience) or with anti-mouse IgM-biotin (Jackson ImmunoResearch) and streptavidin-HRP (R&D Systems) followed by TMB substrate solution (eBioscience). Absorbance was measured at 450 nm.

***In vitro* B cell suppression assay**

Splenic B cells from Vert-X IL-10 reporter mice were isolated by positive selection using CD19-coupled MicroBeads (Miltenyi Biotec) and were cultured for 16h with ultrapure LPS (500 ng/ml) plus addition of PMA (50 ng/ml) and ionomycin (500 ng/ml) during the last 5 h. B cell cultures were surface stained and indicated $CD19^+$ B subpopulations were purified with >98% purities by fluorescence activated cell sorting based on B220 vs. GFP (IL-10) expression. Naïve $CD4^+$ and naïve $CD8^+$ T cells were isolated from C57BL/6J wild type mice by using respective naïve T cell isolation kits (Miltenyi Biotec). For suppression assays, FACS-sorted B cell subpopulations were co-cultured with purified naïve T cells ($3x10^5$ B cells : $6x10^5$ T cells) in 48-well plates that had been pre-coated with anti-CD3 (10µg/ml, clone 145-2C11, eBioscience) for 48 h. During the last 5 h PMA/ionomycin plus Brefeldin A and Monensin was added to the cultures. Cells were subjected to surface and intracellular FACS-staining and analyzed by flow cytometry.

Statistical analysis

Data are presented as mean values ± standard error of the mean (SEM). Statistical analysis was performed using GraphPad Prism (version 6.0h, Mac OS X). Unless stated otherwise, differences between means were assessed using 2-tailed Student's *t* test. Statistical analysis of Kaplan-Meier survival curves was performed by the log-rank test. A *P* value of <0.05 was considered statistically significant. *ns, not significant; *P < 0.05, **P < 0.01, ***P < 0.001.*

Study approval

Animal experiments were performed in accordance with institutional guidelines and were approved by the local authorities (Lower Saxony State Office for Consumer Protection and Food Safety, Germany).

Author contributions

Conceptualization, KH.L.; Methodology, J.Y, VHH.D., G.G. and N.F; Investigation, J.Y, VHH.D., K.W., A.W. and A.S.; Writing – Original Draft, N.F. and KH.L.; Writing – Review and Editing, N.F. and KH.L.; Resources, AC.C and K.B.; Supervision, N.F. and KH.L.; Funding Acquisition, KH.L.

Acknowledgments

We greatly appreciate the excellent technical support of Martina Krautkrämer and Alibek Galeev. We thank Prof. Dr. André Bleich and Dr. Inga Brüsch for providing IL-10-deficient mice. This work was supported by grants from the DFG (LE1254/2-1 and LE1254/2-2) and the Foundation for Pathobiochemistry and Molecular Diagnostics (SPMD).

References

1. Plitas G, Rudensky AY. Regulatory T Cells: Differentiation and Function. *Cancer Immunol Res*. 2016;4(9):721-725.
2. Wolf SD, Dittel BN, Hardardottir F, Janeway CA, Jr. Experimental autoimmune encephalomyelitis induction in genetically B cell-deficient mice. *J Exp Med. 1996*;184(6):2271-2278.
3. Mauri C, Gray D, Mushtaq N, Londei M. Prevention of arthritis by interleukin 10-producing B cells. *J Exp Med.* 2003;197(4):489-501.
4. Evans JG, et al. 2007. Novel suppressive function of transitional 2 B cells in experimental arthritis. *J Immunol*. 2007;178(12):7868-7878.
5. Fillatreau S, Sweenie CH, McGeachy MJ, Gray D, Anderton SM. B cells regulate autoimmunity by provision of IL-10. *Nat Immunol.* 2002;3(10):944-950.
6. Matsushita T, Yanaba K, Bouaziz JD, Fujimoto M, Tedder TF. Regulatory B cells inhibit EAE initiation in mice while other B cells promote disease progression. *J Clin Invest.* 2008;118(10):3420-3430.
7. Mizoguchi A, Mizoguchi E, Takedatsu H, Blumberg RS, Bhan AK. Chronic intestinal inflammatory condition generates IL-10-producing regulatory B cell subset characterized by CD1d upregulation. *Immunity.* 2002;16(2):219-230.
8. Yang M, et al. IL-10-producing regulatory B10 cells ameliorate collagen-induced arthritis via suppressing Th17 cell generation. *Am J Pathol*. 2012;180(6):2375-2385.
9. Lee KM*, et al*. Anti-CD45RB/anti-TIM-1-induced tolerance requires regulatory B cells. *Am J Transplant.* 2012;12(8):2072-2078.
10. Horikawa M, et al. Regulatory B cell (B10 Cell) expansion during Listeria infection governs innate and cellular immune responses in mice. *J Immunol*. 2013;190(3):1158-1168.
11. Inoue S, Leitner WW, Golding B, Scott D. Inhibitory effects of B cells on antitumor immunity. *Cancer Res.* 2006;66(15):7741-7747.
12. Tedder TF. B10 cells: a functionally defined regulatory B cell subset. *J Immunol*. 2015;194(4):1395-1401.
13. Mauri C, Menon M. The expanding family of regulatory B cells. *Int Immunol*. 2015;27(10):479-486.
14. Vire B, David A, Wiestner A. TOSO, the Fcmicro receptor, is highly expressed on chronic lymphocytic leukemia B cells, internalizes upon IgM binding, shuttles to the lysosome, and is downregulated in response to TLR activation. *J Immunol*. 2011;187(8):4040-4050.
15. Pallasch CP, et al. Overexpression of TOSO in CLL is triggered by B-cell receptor signaling and associated with progressive disease. *Blood*. 2008;112(10):4213-4219.
16. Proto-Siqueira R*,* et al. SAGE analysis demonstrates increased expression of TOSO contributing to Fas-mediated resistance in CLL. *Blood*. 2008;112(2):394-397.

17. Hitoshi Y, et al. Toso, a cell surface, specific regulator of Fas-induced apoptosis in T cells. *Immunity*. 1998;8(4):461-471.

18. Nguyen XH, et al. Toso regulates the balance between apoptotic and nonapoptotic death receptor signaling by facilitating RIP1 ubiquitination. *Blood*. 2011;118(3):598-608.

19. Kubagawa H, et al. Identity of the elusive IgM Fc receptor (Fc R) in humans. *J Exp Med*. 2009;206(12):2779-2793.

20. Shima H, et al. Identification of TOSO/FAIM3 as an Fc receptor for IgM. *Int Immunol*. 2010;22(3):149-156.

21. Nguyen TT, et al. The IgM receptor FcμR limits tonic BCR signaling by regulating expression of the IgM BCR. *Nat Immunol*. 2017;18(3):321-333.

22. Ouchida R, et al. FcμR Interacts and Cooperates with the B Cell Receptor To Promote B Cell Survival. *J Immunol*. 2015;194(7):3096-3101.

23. Choi SC, et al. Mouse IgM Fc receptor, FCMR, promotes B cell development and modulates antigen-driven immune responses. *J Immunol*. 2013;190(3):987-996.

24. Honjo K, et al. Altered Ig levels and antibody responses in mice deficient for the Fc receptor for IgM (FcμR). *Proc Natl Acad Sci USA*. 2012;109(39):15882-15887.

25. Ouchida R, et al. Critical role of the IgM Fc receptor in IgM homeostasis, B-cell survival, and humoral immune responses. *Proc Natl Acad Sci USA*. 2012;109(40):E2699-2706.

26. Wang H, Coligan JE, Morse HC, 3rd. Emerging Functions of Natural IgM and Its Fc Receptor FCMR in Immune Homeostasis. *Front Immunol.* 2016;7:99.

27. Lang KS, et al. Involvement of Toso in activation of monocytes, macrophages, and granulocytes. *Proc Natl Acad Sci USA*. 2013;110(7):2593-2598.

28. Lang PA, et al. Toso regulates differentiation and activation of inflammatory dendritic cells during persistence-prone virus infection. *Cell Death Differ*. 2014;22(1):164-173.

29. Brenner D, et al. Toso controls encephalitogenic immune responses by dendritic cells and regulatory T cells. *Proc Natl Acad Sci USA*. 2014;111(3):1060-1065.

30. Thomas PG, Keating R, Hulse-Post DJ, Doherty PC. Cell-mediated protection in influenza infection. *Emerg Infect Dis.* 2006;12(1):48-54.

31. La Gruta NL, Turner SJ. T cell mediated immunity to influenza: mechanisms of viral control. *Trends Immunol.* 2014;35(8):396-402.

32. Sharpe AH, Wherry EJ, Ahmed R, Freeman GJ. The function of programmed cell death 1 and its ligands in regulating autoimmunity and infection. *Nat Immunol.* 2007;8(3):239-245.

33. Grassl GA, Valdez Y, Bergstrom KS, Vallance BA, Finlay BB. Chronic enteric salmonella infection in mice leads to severe and persistent intestinal fibrosis. *Gastroenterology.* 2008;134(3):768-780.

34. Yanaba K, et al. 2008. A regulatory B cell subset with a unique CD1dhiCD5+ phenotype controls T cell-dependent inflammatory responses. *Immunity*. 2008;28(5):639-650.

35. Mauri C, Bosma A. Immune regulatory function of B cells. *Annu Rev Immunol*. 2012;30:221-241.

36. Candando KM, Lykken JM, Tedder TF. B10 cell regulation of health and disease. *Immunol Rev*. 2014;259(1):259-272.

37. Kaku H, Cheng KF, Al-Abed Y, Rothstein TL. A novel mechanism of B cell-mediated immune suppression through CD73 expression and adenosine production. *J Immunol.* 2014;193(12):5904-5913.

38. Casola S. Control of peripheral B-cell development. *Curr Opin Immunol.* 2007;19(2):143-149.

39. Hardy RR, Hayakawa K. Selection of natural autoreactive B cells. *Clin Exp Rheumatol.* 2015;33(4 Suppl 92):S80-86.

40. Pao LI, et al. B cell-specific deletion of protein-tyrosine phosphatase Shp1 promotes B-1a cell development and causes systemic autoimmunity. *Immunity*. 2007;27(1):35-48.

41. Srinivasan L, et al. PI3 kinase signals BCR-dependent mature B cell survival. *Cell*. 2009;139(3):573-586.

42. Sun K, Torres L, Metzger DW. A detrimental effect of interleukin-10 on protective pulmonary humoral immunity during primary influenza A virus infection. *J Virol*. 2010;84(10):5007-5014.

43. McKinstry KK, et al. IL-10 deficiency unleashes an influenza-specific Th17 response and enhances survival against high-dose challenge. *J Immunol*. 2009;182(12):7353-7363.

44. Madan R, et al. Nonredundant roles for B cell-derived IL-10 in immune counter-regulation. *J Immunol*. 2009;183(4):2312-2320.

45. O'Garra A, Chang R, Go N, Hastings R, Haughton G, Howard M. Ly-1 B (B-1) cells are the main source of B cell-derived interleukin 10. *Eur J Immunol.* 1992;22(3):711-717.

46. Watanabe R, et al. Regulatory B cells (B10 cells) have a suppressive role in murine lupus: CD19 and B10 cell deficiency exacerbates systemic autoimmunity. *J Immunol.* 2010;184(9):4801-4809.

47. Blair PA, et al. CD19(+)CD24(hi)CD38(hi) B cells exhibit regulatory capacity in healthy individuals but are functionally impaired in systemic Lupus Erythematosus patients. *Immunity*. 2010;32(1):129-140.

48. Ray A, Basu S, Williams CB, Salzman NH, Dittel BN. A novel IL-10-independent regulatory role for B cells in suppressing autoimmunity by maintenance of regulatory T cells via GITR ligand. *J Immunol.* 2012;188(7):3188-3198.

49. Lundy SK, Fox DA. Reduced Fas ligand-expressing splenic CD5+ B lymphocytes in severe collagen-induced arthritis. *Arthritis Res Ther.* 2009;11(4):R128.

50. Natarajan P, et al. Regulatory B cells from hilar lymph nodes of tolerant mice in a murine model of allergic airway disease are CD5+, express TGF-beta, and co-localize with CD4+Foxp3+ T cells. *Mucosal Immunol.* 2012;5(6):691-701.

51. Shen P, et al. IL-35-producing B cells are critical regulators of immunity during autoimmune and infectious diseases. *Nature*. 2014;507(7492):366-370

52. Bendelac A, Bonneville M, Kearney JF. Autoreactivity by design: innate B and T lymphocytes. *Nat Rev Immunol*. 2001;1(3):177-186.

53. Lee CC, Kung JT. Marginal zone B cell is a major source of Il-10 in Listeria monocytogenes susceptibility. *J Immunol*. 2012;189(7):3319-3327.

54. Bankoti R, Gupta K, Levchenko A, Stäger S. Marginal Zone B Cells Regulate Antigen-Specific T Cell Responses during Infection. *J Immunol*. 2012;188(8):3961-3971.

55. Sindhava V, Woodman ME, Stevenson B, Bondada S. Interleukin-10 mediated autoregulation of murine B-1 B-cells and its role in Borrelia hermsii infection. *PLoS ONE*. 2010;5(7):e11445.

56. Zhang X1, Deriaud E, Jiao X, Braun D, Leclerc C, Lo-Man R. Type I interferons protect neonates from acute inflammation through interleukin 10-producing B cells. *J Exp Med.* 2007;204(5):1107-1118.

57. Shimomura Y, et al. Regulatory role of B-1 B cells in chronic colitis. *Int Immunol.* 2008;20(6):729-737.

58. Miles K, et al. A tolerogenic role for Toll-like receptor 9 is revealed by B-cell interaction with DNA complexes expressed on apoptotic cells. *Proc Natl Acad Sci USA*. 2012;109(3):887-892.

59. Gray M, Miles K, Salter D, Gray D, Savill J. Apoptotic cells protect mice from autoimmune inflammation by the induction of regulatory B cells. *Proc Natl Acad Sci USA*. 2007;104(35):14080-14085.

60. Enghard P, et al. Class switching and consecutive loss of dsDNA-reactive B1a B cells from the peritoneal cavity during murine lupus development. *Eur J Immunol.* 2010;40(6):1809-1818.

61. Takahashi T, Strober S. Natural killer T cells and innate immune B cells from lupus-prone NZB/W mice interact to generate IgM and IgG autoantibodies. *Eur. J. Immunol.* 2008;38(1):156-165.

62. Haas KM, et al. Protective and pathogenic roles for B cells during systemic autoimmunity in NZB/W F1 mice. *J Immunol*. 2010;184(9):4789-4800.

63. Valdez Y, et al. Nramp1 drives an accelerated inflammatory response during Salmonella-induced colitis in mice. *Cell Microbiol.* 2009;11(2):351-362.

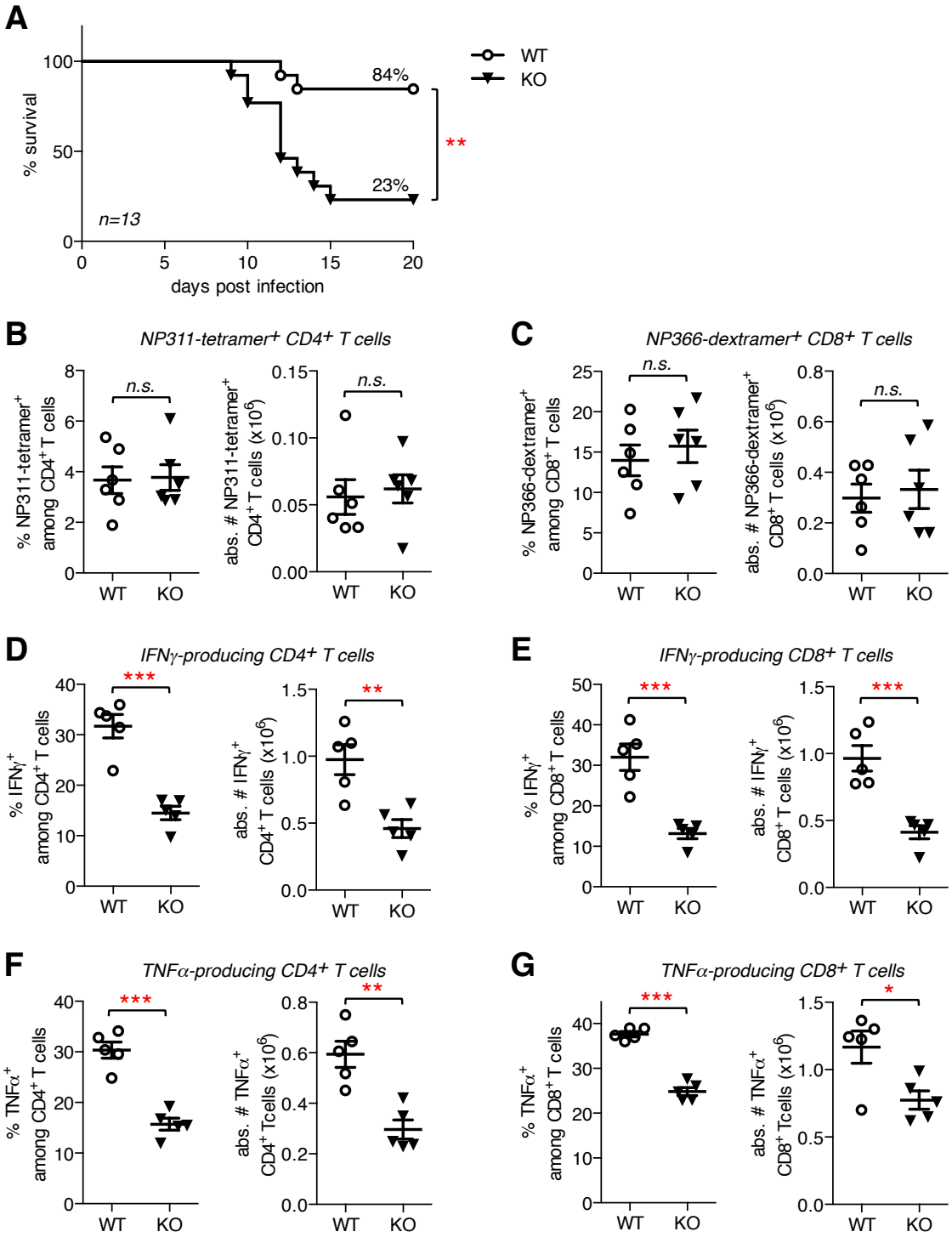

Figure 1. Toso-deficiency results in increased mortality and reduced production of inflammatory cytokines by T cells upon influenza infection.

WT and Toso$^{-/-}$ (KO) mice were infected intranasally with 1000 PFU influenza virus strain A/PR8 (H1N1). (**A**) Survival of mice was monitored over time. n=13 per genotype; ** P<0.005; log-rank test. (**B, C**) Lung cells were isolated at day 9 post infection (*p.i.*) and the frequency and number of virus specific I-A^b/NP$_{311\text{-}325}$ (NP311)-tetramer$^+$ CD4 T cells (**B**) and D^b/NP$_{366\text{-}374}$ (NP366)-dextramer$^+$ CD8 T cells (**C**) was quantified. (**D-G**) Lung cells isolated on day 9 *p.i.*

were restimulated *ex vivo* and number and frequency of IFNγ-producing (**D, E**) and TNFα-producing (**F, G**) $CD4^+$ T cells (**D, F**) and $CD8^+$ T cells (**E, G**) was quantified by intracellular cytokine staining. (**B-G**) Each symbol represents an individual mouse; horizontal line indicates the mean (± SEM). (**B, C**) n=6; (**D-G**) n=5. * P<0.05; ** P<0.01; *** P<0.001; Students t test. Data are representative for at least 4 independent experiments.

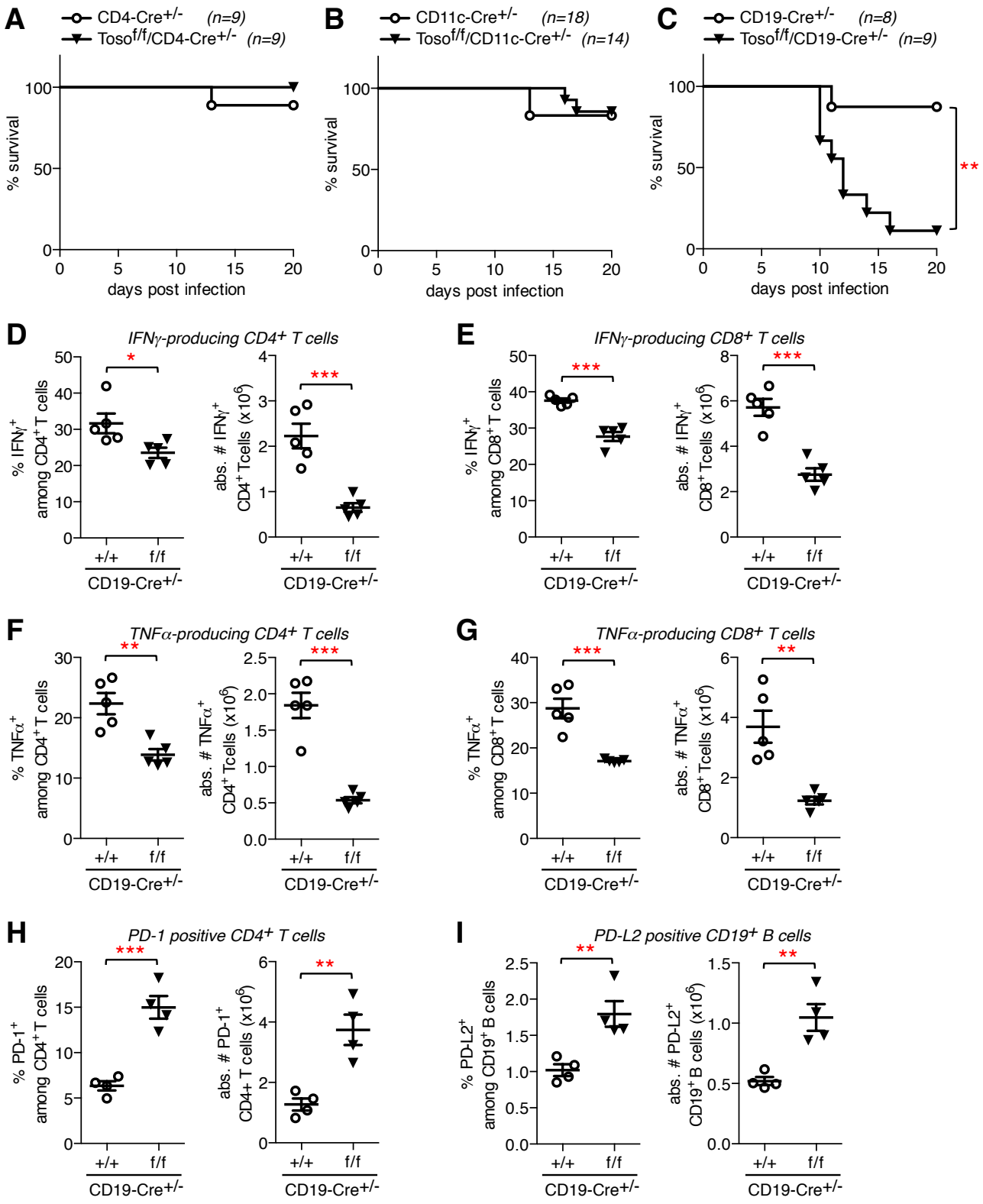

Figure 2. Conditional deletion of Toso in B cells results in increased mortality and reduced T cell cytokine responses upon influenza infection

(**A-G**) Mice were infected intranasally with 1000 PFU influenza virus strain A/PR8 (H1N1). (**A-C**) Survival of mice was monitored over time. (**A**) CD4-Cre$^{+/-}$ and Toso$^{f/f}$/CD4-Cre$^{+/-}$ mice (*n*=9).

(**B**) CD11c-Cre$^{+/-}$ and Toso$^{f/f}$/CD11c-Cre$^{+/-}$ mice (n≥14). (**C**) CD19-Cre$^{+/-}$ mice and Toso$^{f/f}$/CD19-Cre$^{+/-}$ mice. (n≥8). ** P<0.005; log-rank test. (**D-G**) Lung cells isolated on day 9 *p.i.* were restimulated *ex vivo* and number and frequency of IFNγ-producing (**D, E**) and TNFα-producing (**F, G**) CD4$^+$ T cells (**D, F**) and CD8$^+$ T cells (**E, G**) was quantified by intracellular cytokine staining. (**H-I**) CD19-Cre$^{+/-}$ mice and Toso$^{f/f}$/CD19-Cre$^{+/-}$ mice were infected intranasally with 50 PFU influenza virus strain A/PR8 (H1N1). At day 7 *p.i.*, spleens were analyzed for frequency and number of PD-1 positive CD4$^+$ T cells (**H**) and PD-L2 positive CD19$^+$ B cells (**I**). (**D-I**) Each symbol represents an individual mouse; horizontal line indicates the mean (± SEM). (**D-G**) n=5; (**H, I**) n=4. * P<0.05; ** P<0.01; *** P<0.001; Students t test. Data are representative for at least 3 independent experiments.

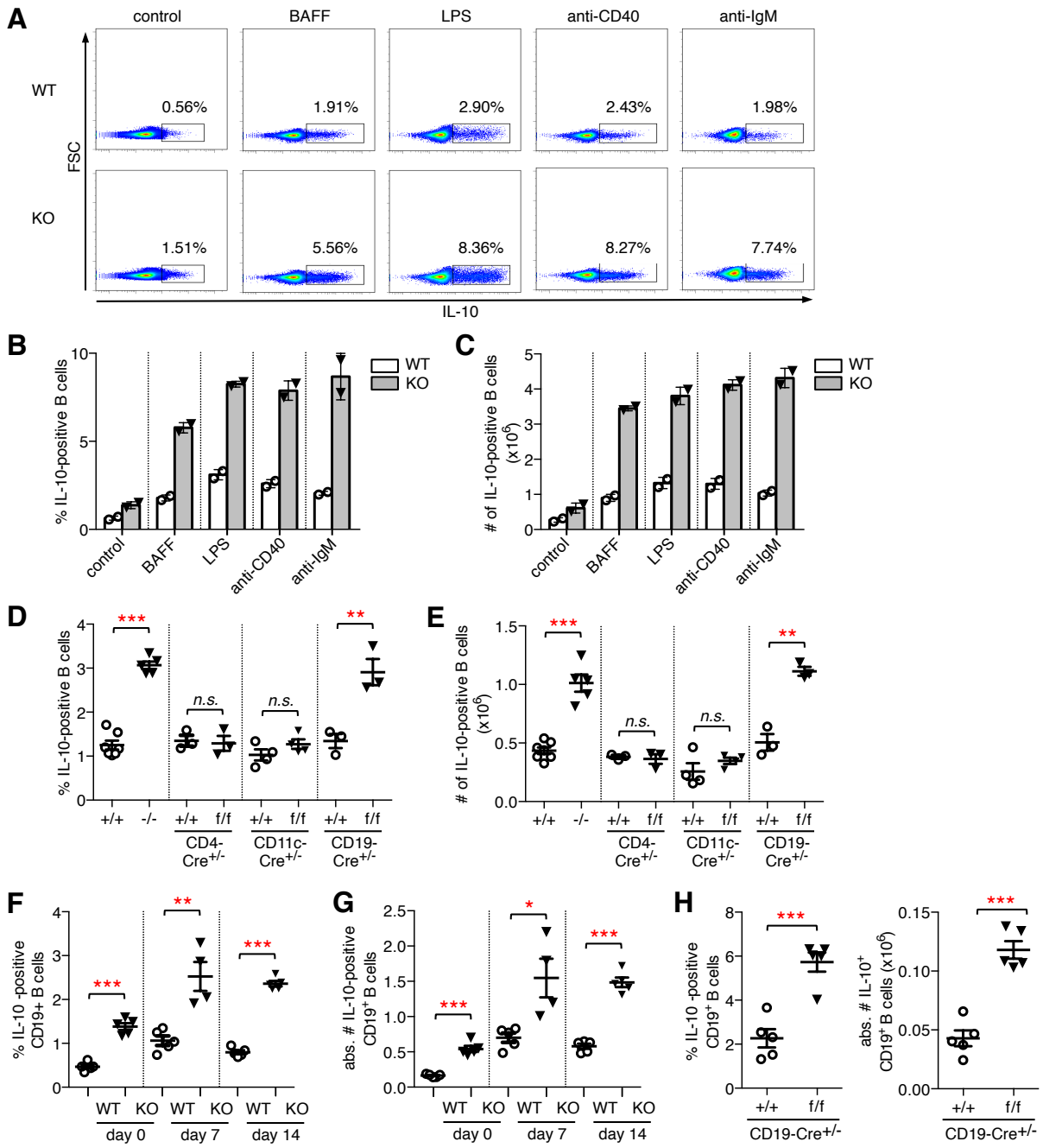

Figure 3. Toso-deficiency results in increased numbers of IL-10-producing B cells.

(**A-C**) Purified B cells form WT and Toso$^{-/-}$ (KO) mice were treated with BAFF, LPS, αCD40 or αIgM for 24 h, respectively. For the last 5 hours, cells were stimulated with PMA/ionomycin in the presence of brefeldin A (BFA)/monensin and subsequently analyzed for IL-10 production. (**A**) Representative flow cytometric analysis. (**B, C**) Bar graphs show frequency (**B**) and absolute numbers (**C**) of IL-10-positive B cells. Data are mean ± SEM from 2 cultures derived from different mice. (**D, E**) B cells from straight and conditional Toso knock-out mice, as well as the indicated control mice were stimulated for 5 h with LPS and PMA/ionomycin in the presence of BFA/monensin. Frequency (**D**) and number (**E**) of IL-10-positive B cells was determined by intracellular cytokine staining. (**F, G**) WT and Toso$^{-/-}$ (KO) mice were infected intranasally with 50 PFU influenza virus strain A/PR8 (H1N1). At the indicated days post infection, splenocytes

were restimulated *ex vivo* and the frequency (**F**) and number (**G**) of IL-10-positive $CD19^+$ B cells was quantified by intracellular cytokine staining. (**H**) CD19-$Cre^{+/-}$ mice and $Toso^{f/f}$/CD19-$Cre^{+/-}$ mice were infected intranasally with 1000 PFU influenza virus strain A/PR8 (H1N1). Lung cells isolated on day 9 *p.i.* were restimulated *ex vivo* and number and frequency IL-10-positive $CD19^+$ B cells was quantified by intracellular cytokine staining. Each symbol represents an individual mouse; horizontal line indicates the mean (± SEM). (**D, E**) n= 3-7; (**F-H**) n= 4-5. ** P<0.01; *** P<0.001; Students t test. Data are representative for at least 3 independent experiments.

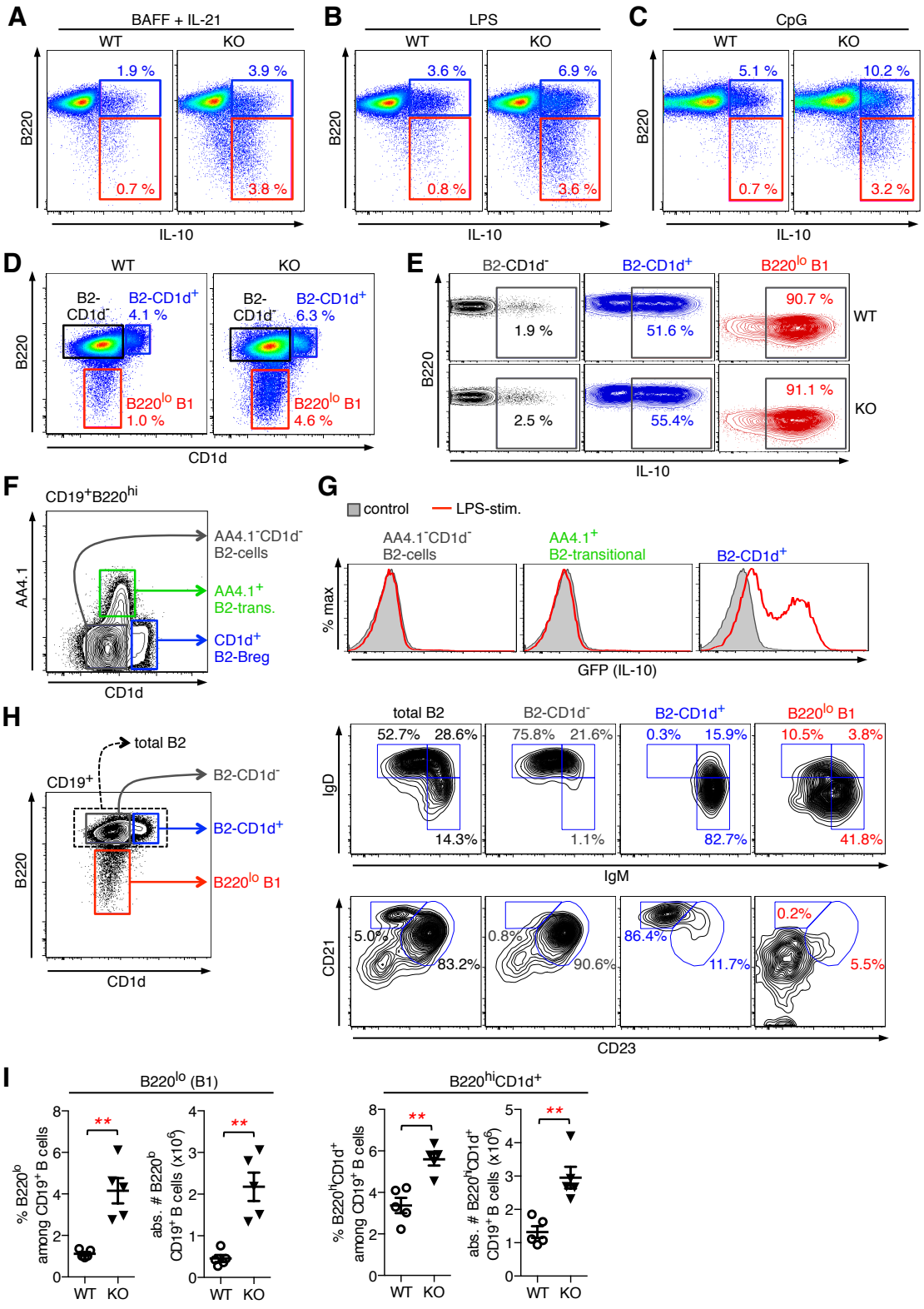

Figure 4. Phenotypic characteristics of IL-10-competent B cell subsets

(**A-C**) Purified B cells from WT and Toso$^{-/-}$ (KO) mice were cultured for 16h with (**A**) BAFF + IL-21, (**B**) LPS or (**C**) CpG oligonucleotides. For the last 5 hours, cells were treated with PMA/ionomycin in the presence of BFA/monensin and CD19^{+} B cells analyzed for IL-10

production. (**D**) B220 vs CD1d staining on naïve $CD19^+$ B cells from WT and $Toso^{-/-}$ (KO) mice. (**E**) $B220^{hi}$ B2-$CD1d^-$ B cells (black), $B220^{hi}$ B2-$CD1d^+$ B cells (blue) and $B220^{lo}$ B1 B cells (red) from WT and $Toso^{-/-}$ (KO) mice were purified by fluorescence activated cell sorting. Cells were stimulated for 16h with LPS plus PMA/ionomycin/BFA/monensin during the last 5 h and subsequently analyzed for IL-10 production. (**F**) $CD19^+B220^{hi}$ B cells were analyzed for CD1d vs AA4.1 (CD93) staining to identify $AA4.1^-CD1d^-$ B2-effector cells, $AA4.1^+$ transitional B2 cells (B2-trans.) and $CD1d^+$ B2-Bregs. (**G**) $AA4.1^-CD1d^-$ B2-effector cells, $AA4^+$ B2-transitional cells and $CD1d^+$ B2-Bregs were purified from IL-10/GFP reporter (Vert-X) mice by flow cytometric cell sorting. Cells were treated for 16h with LPS plus PMA/ionomycin during the last 5 hours and analyzed for GFP (IL-10) expression. (**H**) Flow cytometric analysis of naïve B cells from C57BL/6J mice. Left panel is gated on $CD19^+$ B cells and shows gating for total B2 cells ($B220^{hi}$), $B220^{hi}CD1d^-$ B2 cells, $B220^{hi}CD1d^+$ B2 cells and $B220^{lo}$ B1 cells. FACS profiles on the right show expression IgM vs IgD (upper panel) and CD23 vs CD21 (lower panel) on the indicated B cell subsets. (**I**) Number and frequency of splenic $B220^{lo}$ B1 B cells and $B220^{hi}CD1d^+$ B2 B cells in WT and $Toso^{-/-}$ (KO) mice. Each symbol represents an individual mouse; horizontal line indicates the mean (± SEM). n=5. ** P<0.01; *** P<0.001; Students t test. Data are representative for at least 3 independent experiments.

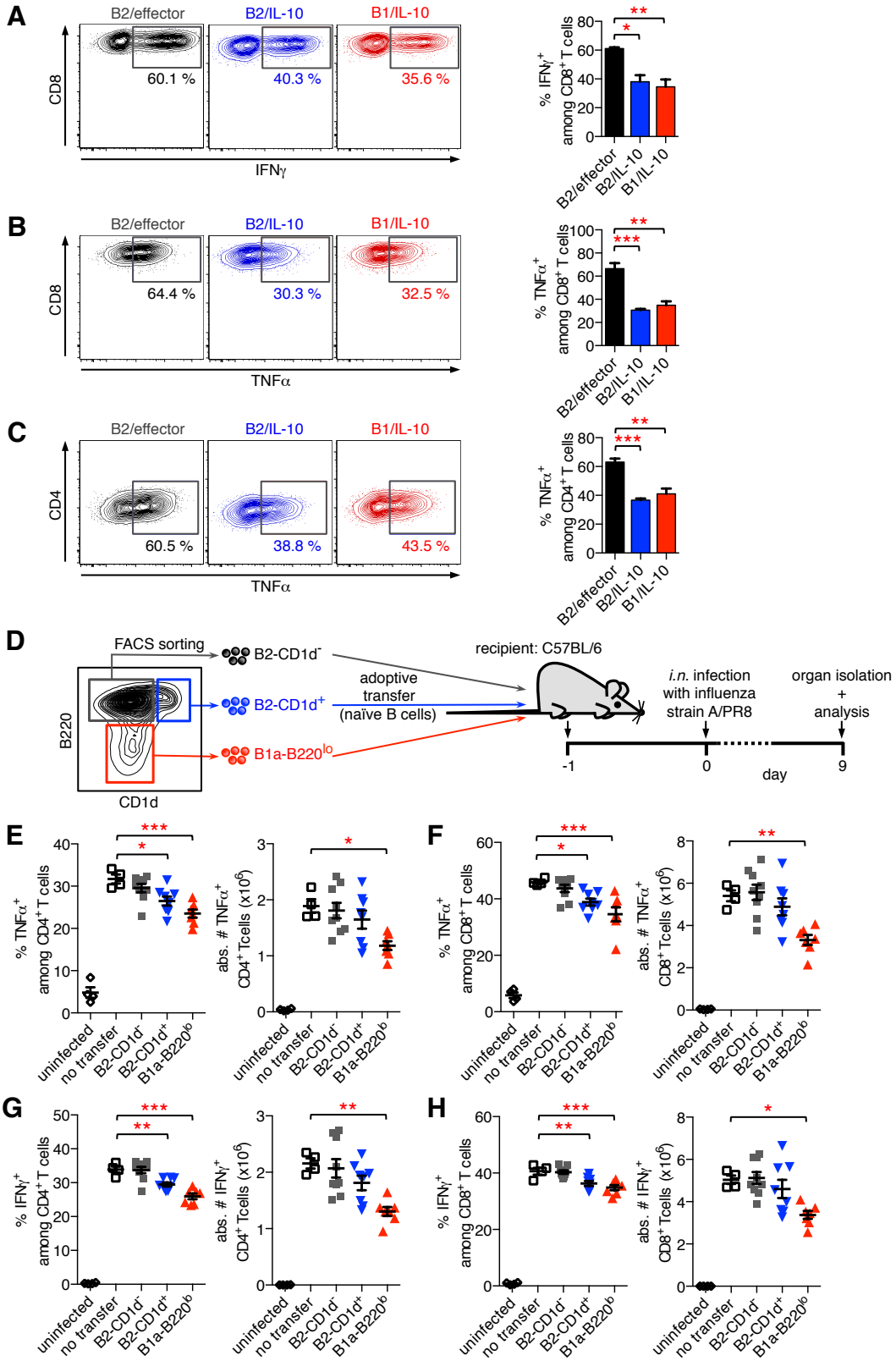

Figure 5. Suppressive function of IL-10-producing regulatory B cells

(**A-C**) Regulatory B cells suppress inflammatory cytokine production in T cells *in vitro*. B cells from IL-10/GFP reporter (Vert-X) mice were treated for 16h with LPS and PMA/ionomycin was

added during the last 5 hours. B2/effector cells ($B220^{hi}GFP^{-}$) B2/IL-10 cells ($B220^{hi}GFP^{+}$) and B1/IL-10 cells ($B220^{lo}GFP^{+}$) were then purified by fluorescence activated cell sorting and were subsequently co-cultured with (**A, B**) naïve CD8 T cells or (**C**) naïve CD4 T cells. Cultures were stimulated with anti-CD3 for 48 h and restimulated with PMA/ionomycin in the presence of BFA/monensin for 5h. Percentage of (**A**) IFNγ- and (**B, C**) TNFα-producing T cells was determined by intracellular cytokine staining. (**D-H**) Regulatory B cells suppress inflammatory cytokine production in T cells during anti-viral immune response *in vivo*. (**D**) Experimental model. Briefly, naïve $CD19^{+}B220^{hi}CD1d^{-}$ B2 B cells (gray), $CD19^{+}B220^{hi}CD1d^{+}$ B2 B cells (blue) and $CD19^{+}B220^{lo}$ B1a cells (red) were purified from $Toso^{-/-}$ (KO) mice by fluorescence activated cell sorting and were adoptively transferred into C57BL/6J mice. Mice were infected intranasally with 1000 PFU influenza virus strain A/PR8 (H1N1). On day 9 *p.i.* lung cells were isolated and analyzed for cytokine staining. (**E-H**) Number and frequency of TNFα-producing (**E, F**) and IFNγ-producing (**G, H**) $CD4^{+}$ T cells (**E, G**) and $CD8^{+}$ T cells (**F, H**). Mice that had not received adoptively transferred cells (=no transfer; open squares), but were also infected with influenza were used as positive control; uninfected mice served as a negative control (open circles). Data are expressed as mean ± SEM; symbols represent individual mice. (**A-C**) n=3; (**E-H**) n= 4-9. * P<0.05; ** P<0.01; *** P<0.001; one-way ANOVA and Dunnett's post-hoc test. Data are representative for at least 3 independent experiments.

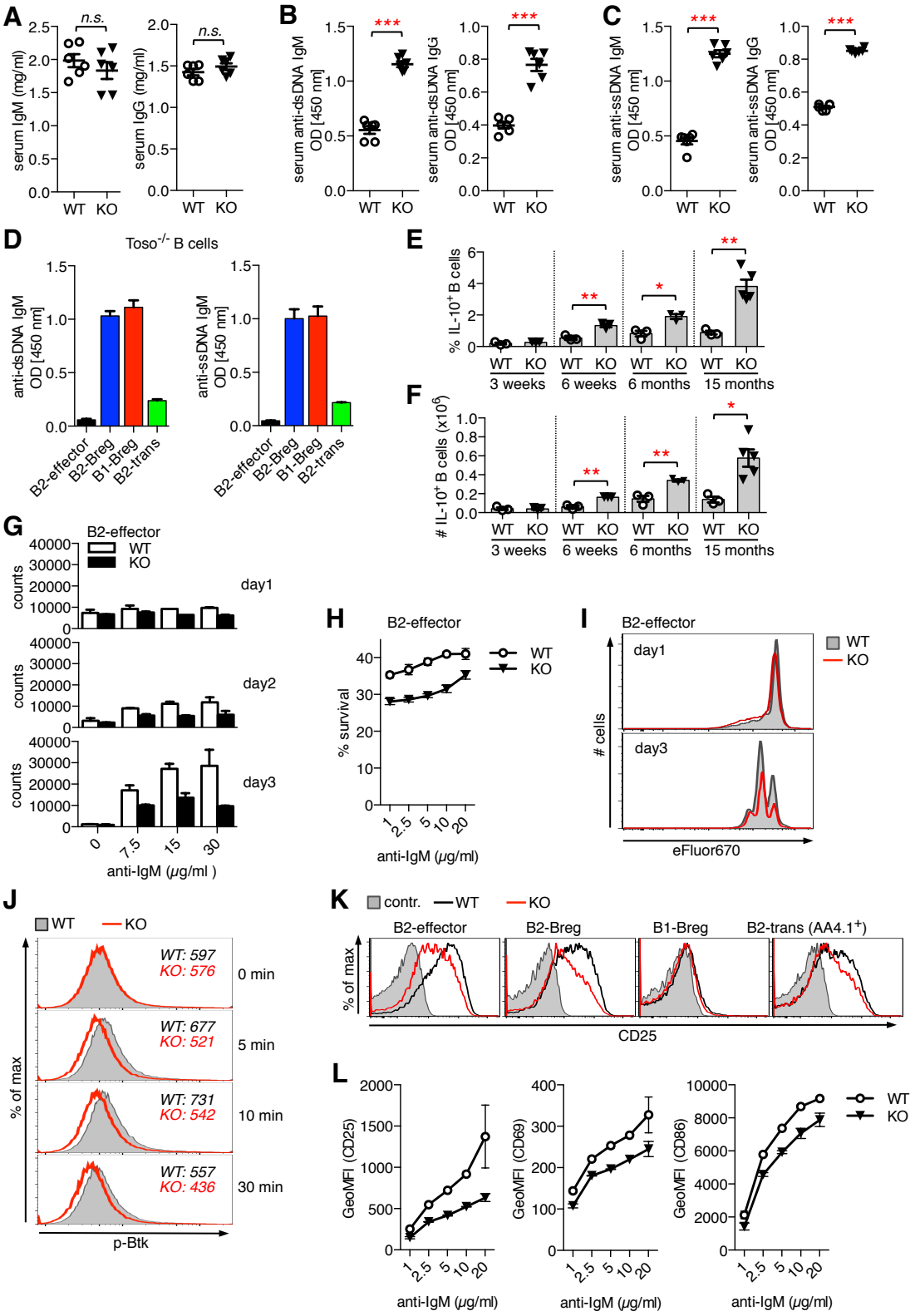

Figure 6. Self-reactivity of regulatory B cell subsets and altered activation thresholds of Toso-deficient B cells

(**A-C**) Serum from 8-10 months old female WT and Toso$^{-/-}$ (KO) mice was analyzed for (**A**) total IgM and IgG levels and (**B, C**) titers of IgM and IgG antibodies against (**B**) dsDNA and (**C**)

ssDNA. *n*=6. (**D, G-L**) Splenic $B220^{hi}AA4.1^{-}CD1d^{-}$ B2-effector cells, $B220^{hi}CD1d^{+}$ B2-Bregs, $B220^{hi}AA4.1^{+}$ B2-transitional cells (B2-trans) and/or $B220^{lo}$ B1-Bregs from $Toso^{-/-}$ mice were purified by fluorescence activated cell sorting. (**D**) Cells were treated for 3 days with LPS. Culture supernatants were analyzed for anti-dsDNA and anti-ssDNA IgM levels (*n*=2). (**E, F**) Splenic B cells from WT and $Toso^{-/-}$ mice of the indicated age were restimulated *ex vivo* and (**E**) frequency and (**F**) numbers of IL-10-positive $CD19^{+}$ B cells was quantified by intracellular cytokine staining. (**G, H**) Sorted $CD19^{+}B220^{hi}AA4.1^{-}CD1d^{lo}$ B2-effector cells from WT and $Toso^{-/-}$ (KO) mice were stimulated for the indicated times with titrated amounts of anti-IgM and analyzed by flow cytometry for (**G**) cell counts (*n*=2) and (**H**) cell survival (*n*=4). (**I**) Sorted B2-effector cells were labeled with eFluor670, stimulated with anti-IgM and analyzed for cell division by measuring eFluor670 dilution. (**J**) Sorted B2-effector cells from WT (gray filled) and $Toso^{-/-}$ (KO) (red line) mice were stimulated for the indicated times with anti-IgM and analyzed for phospho (p)-Btk staining. (**K, L)** Sorted B cell subsets were stimulated for 16h with anti-IgM and analyzed by flow cytometry for upregulation of B cell activation markers. (**K**) Representative flow cytometric histograms for CD25 expression. WT (black); $Toso^{-/-}$ (KO) (red line); unstimulated control (gray filled). (**L**) Sorted $AA4.1^{-}CD1d^{-}$ B2-effector cells were analyzed for anti-IgM induced upregulation of CD25, CD69 and CD86. Data show GeoMFI (*n*=2). (**E, F**) *n*= 3-5. Data are expressed as mean ± SEM. * $P<0.05$; ** $P<0.01$; Students *t* test. All data are representative for 2 - 4 independent experiments.

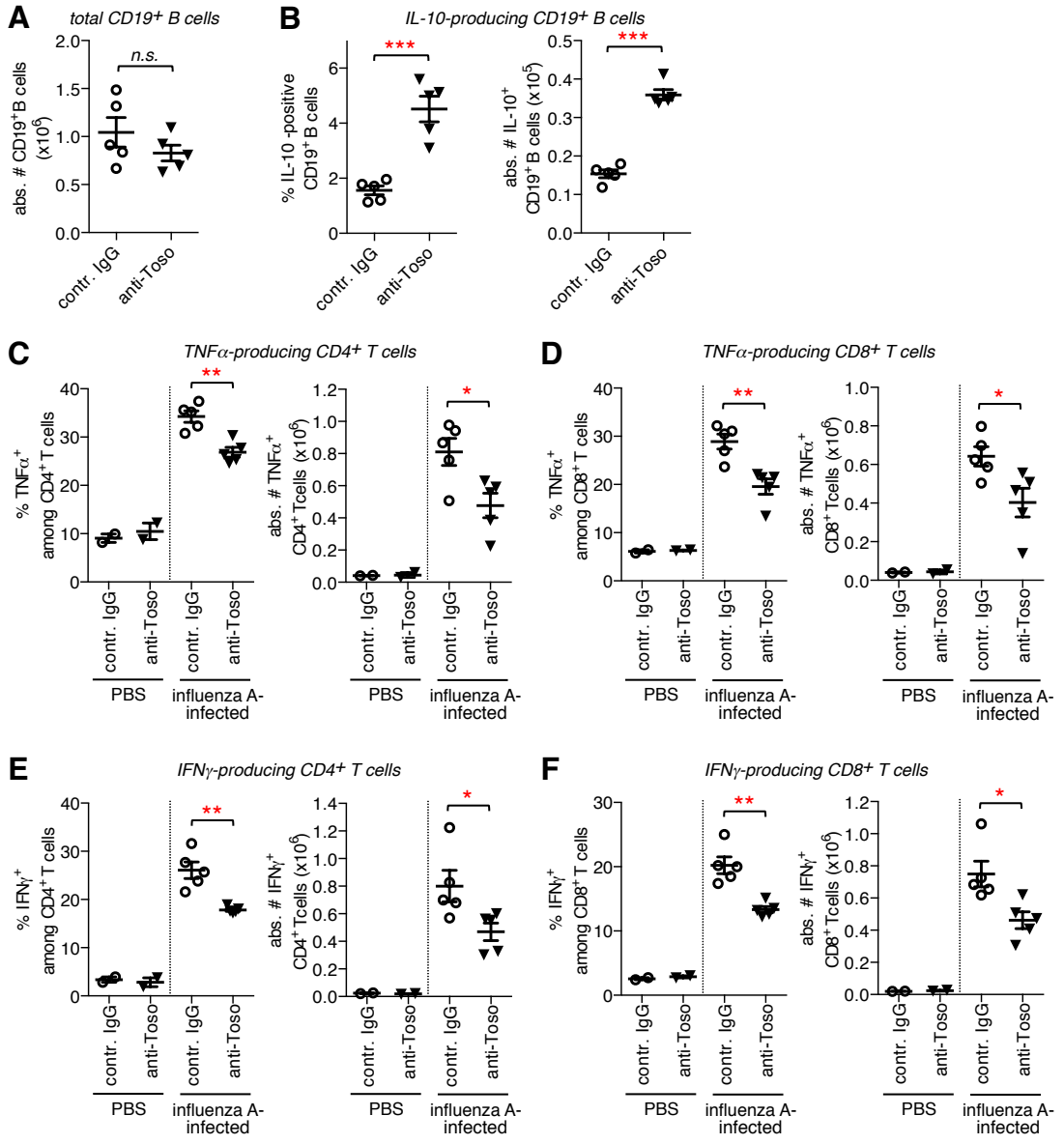

Figure 7. Immunomodulatory effect of Toso-blocking antibody treatment on influenza-induced lung inflammation

Mice were infected intranasally with influenza virus strain A/PR8 (H1N1) to induce pulmonary inflammation. On day -1, day 2 and day 5 *p.i.* mice were treated with anti-Toso mAb or control IgG (200 µg/mouse; *i.v.*). Lung cells isolated on day 9 *p.i.* were restimulated *ex vivo* and analyzed for cytokine production in T and B cells by intracellular cytokine staining. (**A**) Quantification of total CD19-positive B cells and (**B**) frequency and (**C**) number of IL-10-positive B cells in lungs of infected animals. (**C-F**) Quantification of frequency and numbers of (**C, D**) TNFα-producing and (**E, F**) IFNγ-producing $CD4^+$ T cells (**C, E**) and $CD8^+$ T cells (**D, F**). (**A-F**) Each symbol represents an individual mouse; horizontal line indicates the mean (± SEM). PBS control: n=2; influenza A-infected mice: n=5. * P<0.05; ** P<0.01; *** P<0.001; Students t test. Data are representative for 2 independent experiments.

Supplemental Table 1

Description of fluorescent-labeled antibodies used in the study:

antibody specificity	clone	fluorophore(s)	source
CD1d	1B1	FITC, PE, APC, PerCPCy5.5	Biolegend
CD4	GK1.5	Brilliant Violet 510, PerCPCy5.5, Fitc	Biolegend
CD5	53-7.3	APC, PerCPCy5.5	Biolegend
CD8a	53-6.7	Brilliant Violet 510, PerCPCy5.5, PE	Biolegend
CD19	6D5	Brilliant Violet 510	Biolegend
CD21/CD35	7E9	Alexa488, PerCPCy5.5, APC	Biolegend
CD23	B3B4	PE	eBioscience
CD25	PC61.5	PE, APC	eBioscience
CD43	R2/60	PE, APC	eBioscience
CD44	IM7	Fitc, PE, APC	Biolegend
CD62L	MEL-14	PE, APC	Biolegend
CD69	H1.2F3	Alexa488, APC	Biolegend
CD73	TY/11.8	PE, APC	Biolegend
CD80	16-10A1	PE, APC	Biolegend
CD86	GL-1	PE, APC	Biolegend
CD93	AA4.1	PE, APC	Biolegend
CD95 (Fas)	15A7	Alexa488, PE	eBioscience
CD178 (FasL)	MFL3	PE, APC	Biolegend
CD138	281-2	PE, APC	Biolegend
CD178	MFL3	PE, APC	eBioscience
B220	RA3-6B2	Brilliant Violet 510, PerCPCy5.5, APC	Biolegend
F4/80	BM8	PerCPCy5.5, Alexa 488, APC	eBioscience
GL7	GL7	PE	eBioscience
IgD	11-26c.2a	Alexa 488, APC	Biolegend
IgM	RMM-1	PE, APC, PerCPCy5.5	eBioscience
MHCII	M5/114.15.2	PE	Biolegend
NK1.1	PK136	PerCPCy5.5, Alexa 488, APC	Biolegend
PD-1	J43	PE, APC	eBioscience
PD-L2	112	PE, APC	eBioscience
Tim-1	RMT1-4	PE	Biolegend
TNFα	MP6-XT22	Alexa 488, APC	Biolegend
IFNγ	XMG1.2	PE, APC	Biolegend
IL-10	JES5-16E3	PE, APC	Biolegend

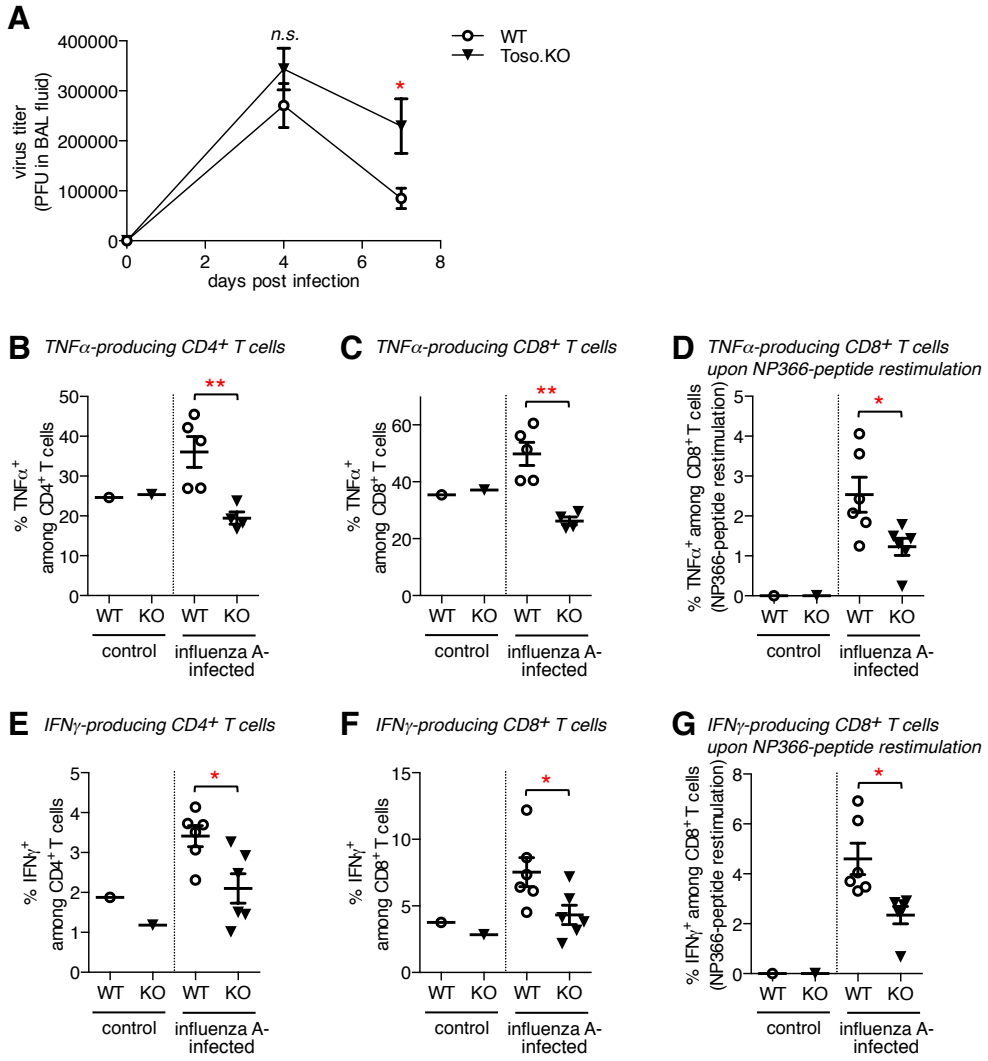

Supplemental Figure 1. Toso-deficiency results in reduced production of inflammatory cytokines by splenic T cells upon influenza infection.

(**A**) Viral titer kinetics in the BAL fluid of WT and Toso$^{-/-}$ (KO) mice infected intranasally with 1000 PFU influenza virus strain A/PR8 (H1N1). day4: n=5; day9: n=10. (**B-G**) WT and Toso$^{-/-}$ (KO) mice were infected intranasally with 50 PFU influenza virus strain A/PR8 (H1N1) (n= 4-6) or control treated. On day 7 post infection splenocytes were restimulated *ex vivo* and number and frequency of TNFα-producing (**B-D**) and IFNγ-producing (**E-G**) CD4$^+$ T cells (**B, E**) and CD8$^+$ T cells (**C, D, F, G**) was quantified by intracellular cytokine staining. (**D, G**) Cells were restimulated with NP366-peptide, an H-2K^b restricted CD8 T cell epitope of influenza A virus nucleoprotein (peptide comprises amino acids 366-374). Each symbol represents an individual mouse; horizontal line indicates the mean (± SEM). * P<0.05; ** P<0.01; Students t test. Data are representative for at least 3 independent experiments.

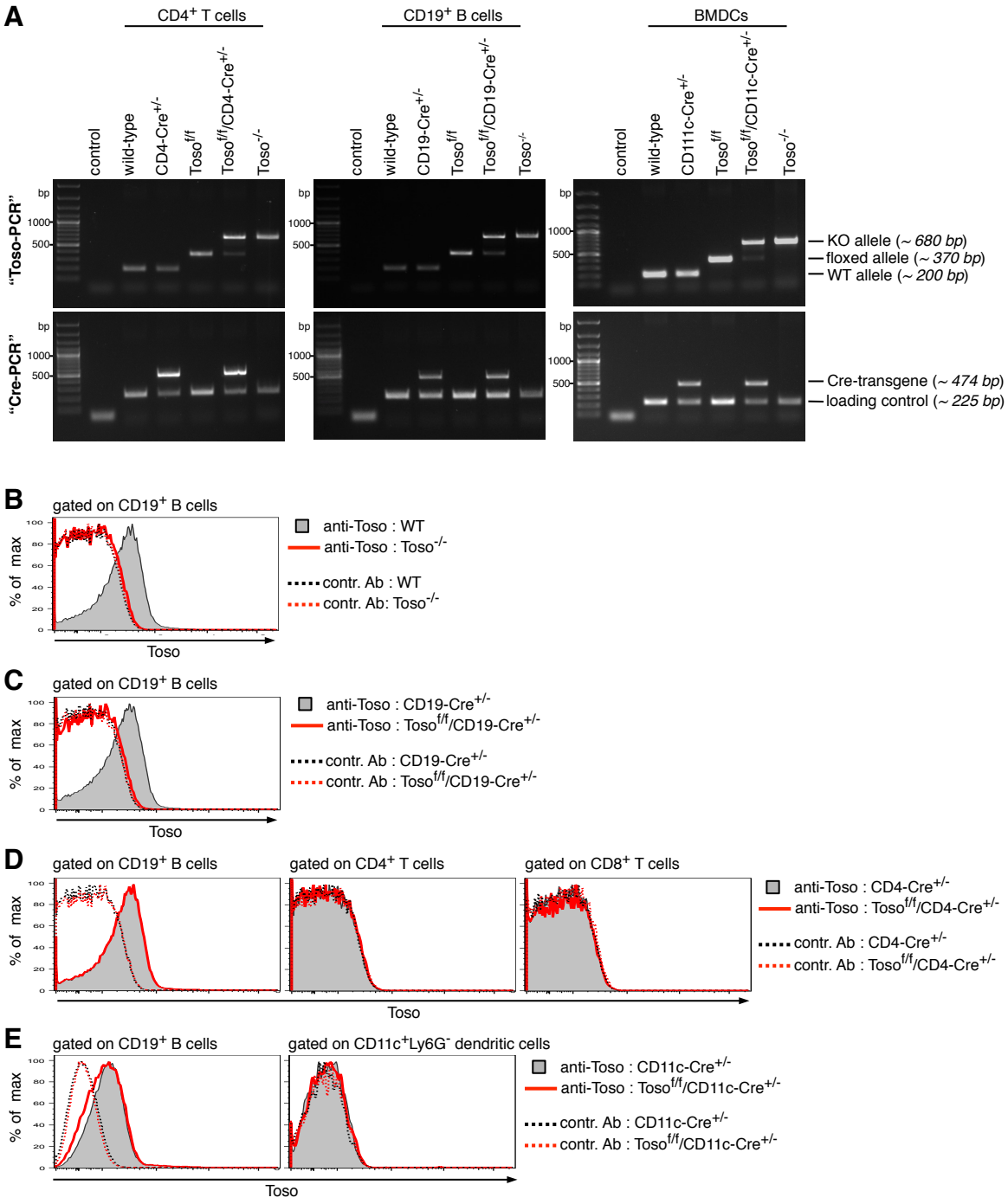

Supplemental Figure 2. Cell type-specific conditional deletion of Toso.

(**A**) PCR genotyping for Toso (upper panel) and Cre-transgene (lower panel). Splenic CD4$^+$ T cells (left panel), and CD19$^+$ B cells (middle panel) were isolated from the indicated mice by positive selection using magnetic-bead purification (Miltenyi Biotec). Right panel shows data for bone marrow-derived dendritic cells (BMDCs). Genomic DNA was isolated from respective cell types and subjected to PCR analysis. Upper panel: PCR primers specifically recognize the wild-type (WT) allele, the floxed Toso allele and the Toso knock-out (KO) allele. Primer sequences: primer#intron7s, 5'-GGCGCTGCAAAATCTGTGGTTATC-3'; primer#intron7as, 5'-GAAATACCTCTCTCACAGAGG-3'; primer#intron3s, 5'-AGCTCTTCTGGAGTCATAGC-3'.

Lower panel: primers are specific for the Cre-transgene and additional primers recognize sequences within the unrelated coronin1a gene locus as a loading control. Primer sequences were: Cre-Tg: primer#Cre-sense, 5'-CCAATTTACTGACCGTACACC-3' and primer#Cre-antisense, 5'- TTACGTATATCCTGGCAGCG-3; loading control: primer#coro1aEx3s, 5'-GTCCACACAATGACAATGTC-3' and primer#coro1aEx4as, 5'-GATGCCAACCCTCTTGGTGT-3'. The size of the expected PCR products is indicated. (**B-E**) Flow cytometric histograms showing Toso-surface expression on the indicated immune cell types from mice of the indicated genotype. Cells were stained with either anti-Toso antibody (grey filled and red line) or isotype matched control antibody (dotted lines).

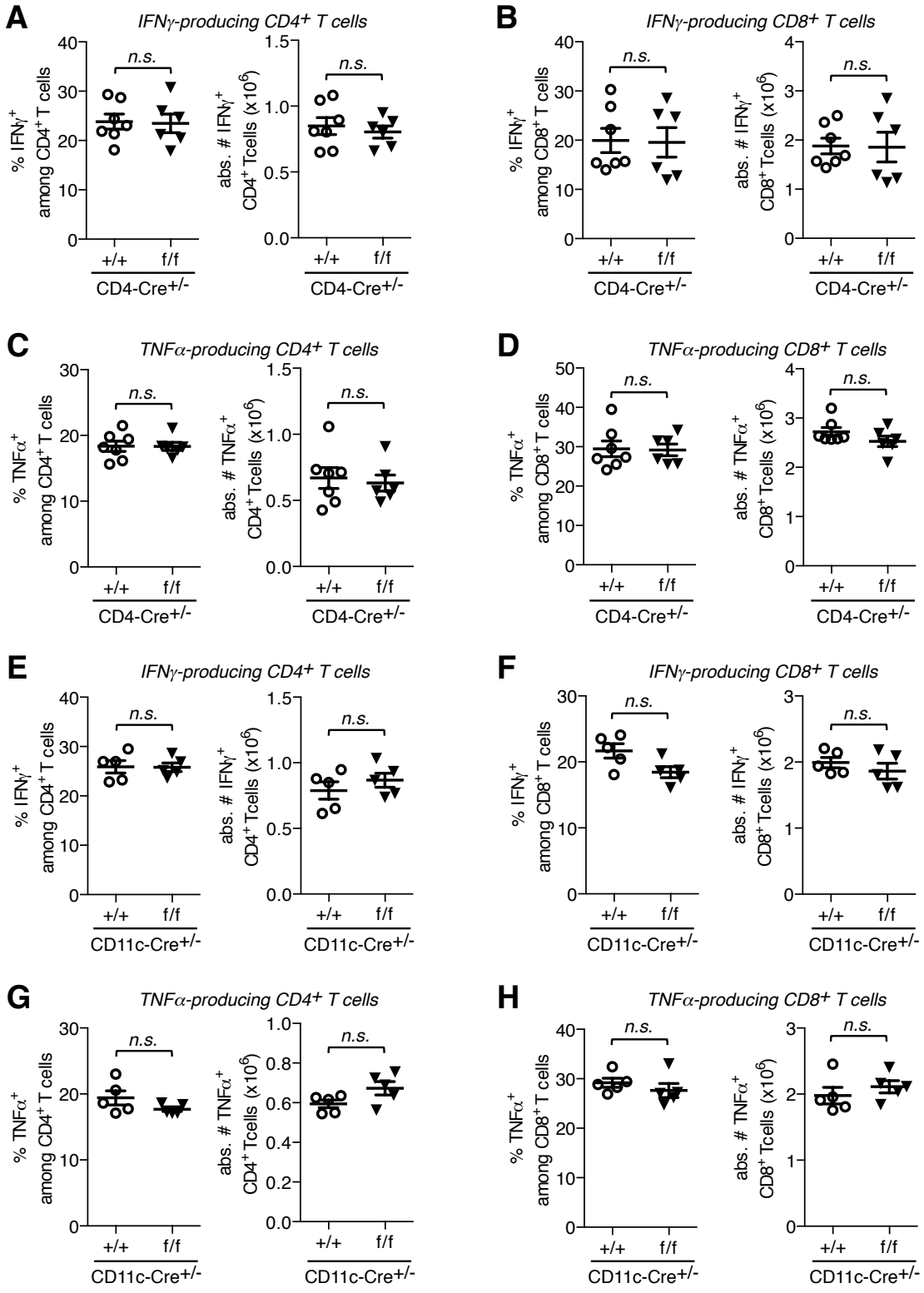

Supplemental Figure 3. Normal influenza-induced T cell cytokine responses upon conditional deletion of Toso in T cells or dendritic cells.

Mice were infected intranasally with 1000 PFU influenza virus strain A/PR8 (H1N1). (**A-D**) CD4-Cre$^{+/-}$ and Toso$^{f/f}$/CD4-Cre$^{+/-}$ mice (n= 6-7), (**E-H**) CD11c-Cre$^{+/-}$ and Toso$^{f/f}$/CD11c-Cre$^{+/-}$ mice (n=5). On day 9 post infection lung cells were isolated and restimulated *ex vivo.* Number

and frequency of IFNγ-producing (**A, B, E, F**) and TNFα-producing (**C, D, G, H**) $CD4^+$ T cells (**A, C, E, G**) and $CD8^+$ T cells (**B, D, F, H**) was quantified by intracellular cytokine staining. Each symbol represents an individual mouse; horizontal line indicates the mean (± SEM). *n.s.,* not significant; Students *t* test. Data are representative for at least 2 independent experiments.

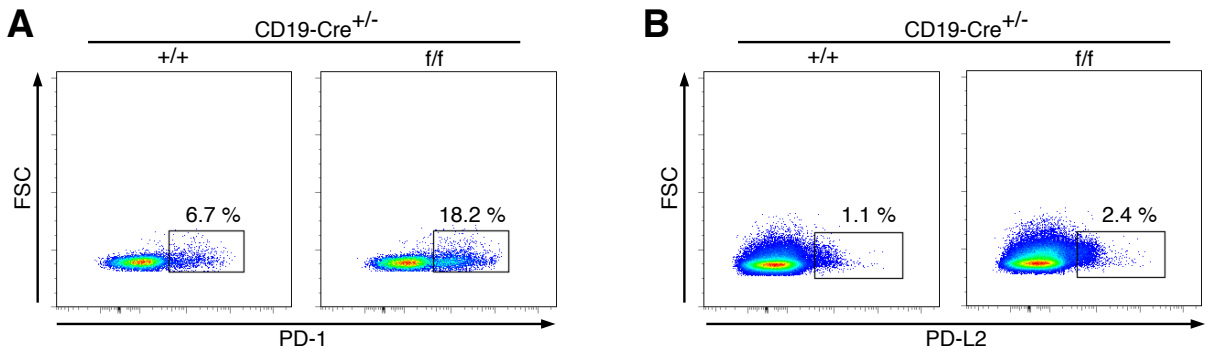

Supplemental Figure 4. Enhanced expression of PD-1 and PD-L2 in Toso$^{f/f}$/CD19-Cre$^{+/-}$ mice during influenza infection

CD19-Cre$^{+/-}$ mice and Toso$^{f/f}$/CD19-Cre$^{+/-}$ mice were infected intranasally with 50 PFU influenza virus strain A/PR8 (H1N1) and spleens were analyzed at day 7 *p.i.*. (**A, B**) Representative flow cytometric analysis showing (**A**) PD-1 staining on CD4-positive splenic T cells and (**B**) PD-L2 staining on CD19-positive splenic B cells.

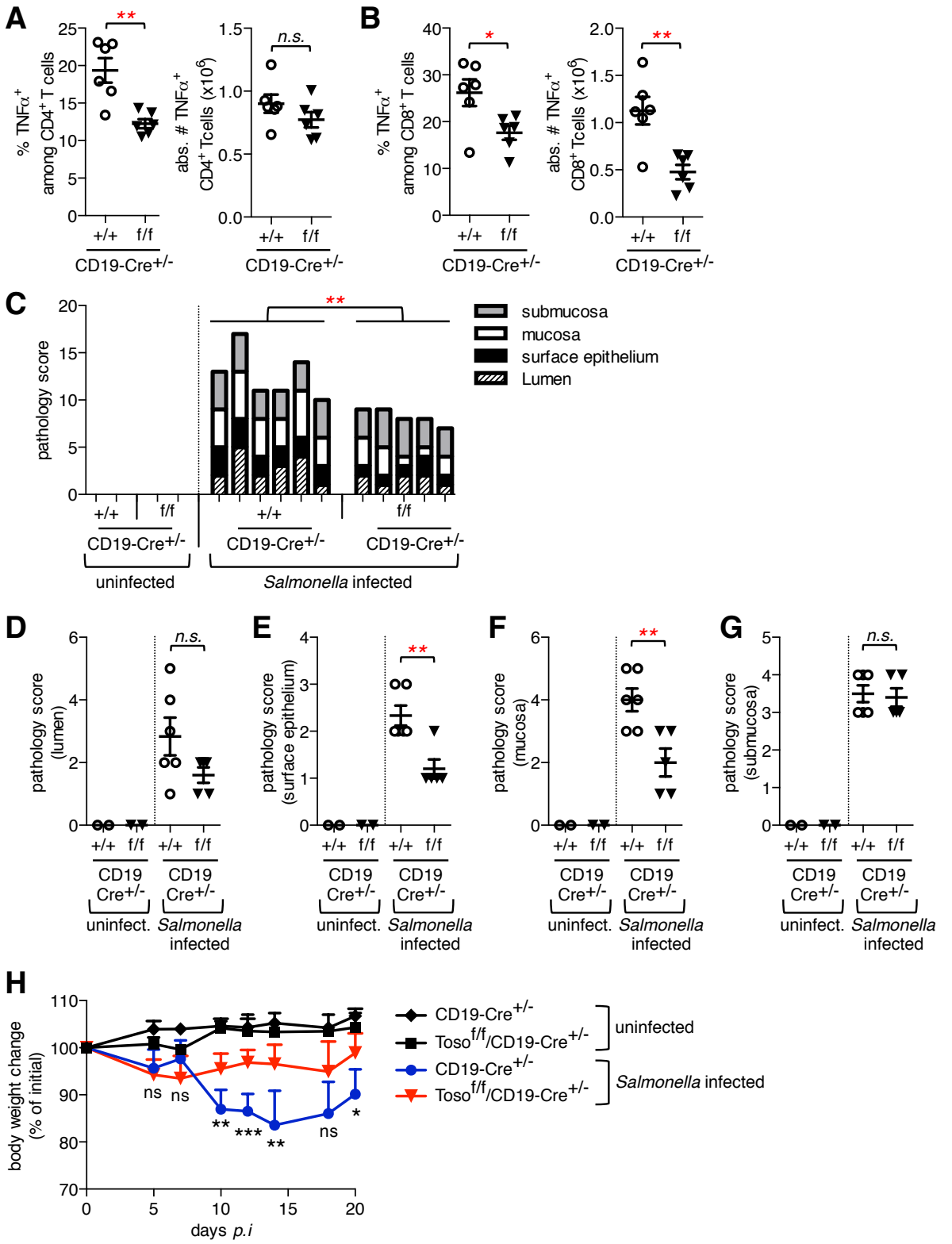

Supplemental Figure 5. Reduced immunopathology upon conditional deletion of Toso on B cells in a model of chronic bacterial-induced colitis

CD19-Cre$^{+/-}$ mice and Toso$^{f/f}$/CD19-Cre$^{+/-}$ mice were orally infected with *S.* Typhimurium *ΔaroA* at a dose of 3 × 10^6 bacteria. (**A, B**) On day 7 *p.i.* spleen cells were restimulated *ex vivo* and

number and frequency of TNFα-producing (**A**) $CD4^+$ T cells and (**B**) $CD8^+$ T cells was quantified by intracellular cytokine staining. (**C-G**) Pathology score of infected ceca analyzed at day 7 *p.i.* (**C**) Total cecal pathology score and pathology scores of (**D**) lumen, (**E**) surface epithelium, (**F**) mucosa, and (**G**) submucosa. Pathological scores were determined as follows: Lumen. empty [0], necrotic epithelial cells scant [1]; moderate [2]; dense [3], and neutrophils scant [1]; moderate [2]; dense [3]. Surface epithelium. no pathological changes [0]; desquamation, patchy [1] or diffuse [2], ulceration [1]. Mucosa. no pathological changes [0]; crypt abscesses: rare [1], moderate [2], or abundant [3]; inflammatory infiltrate: rare [1], moderate [2], or abundant [3]; lymphocyte aggregates: rare [0], moderate [1], or abundant [2]. Submucosa. no pathological changes [0]; lymphocyte aggregates: rare [0], moderate [1], or abundant [2]; neutrophils: none [0], moderate [1], or abundant [2]; edema: moderate [1], or severe [2]. (**A-G**) Each symbol represents an individual mouse; horizontal line indicates the mean (± SEM). *Salmonella*-infected mice: n= 5-6; Students t-test. (**H**) Chronic Salmonella infection-associated change in body weight was monitored over time. Data are expressed as percent of initial body weight. Uninfected: n= 2-3; *Salmonella*-infected: n= 5-6. * $P<0.05$; ** $P<0.01$; *** $P<0.001$; one-way ANOVA and Tukey's post test.

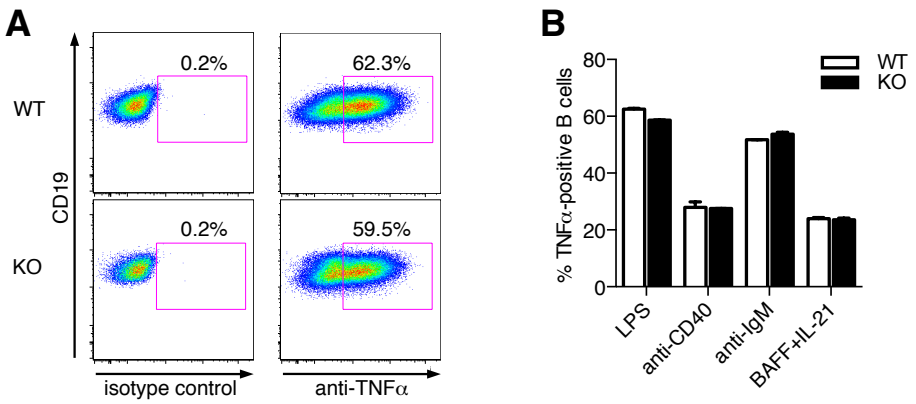

Supplemental Figure 6. Analysis of TNFα-production in Toso-deficient B cells

(**A, B**) Purified B cells form WT and Toso$^{-/-}$ (KO) mice were treated with LPS, αCD40, αIgM or BAFF+IL21 for 24 h, respectively. For the last 5 hours, cells were stimulated with PMA/ionomycin in the presence of brefeldin A (BFA)/monensin and TNFα production was subsequently analyzed by intracellular cytokine staining. (**A**) Representative flow cytometric analysis of LPS-treated B cells (**B**) Bar graph shows frequency of TNFα-positive B cells. Data are mean ± SEM from 2 cultures derived from different mice. Data are representative for 2 independent experiments.

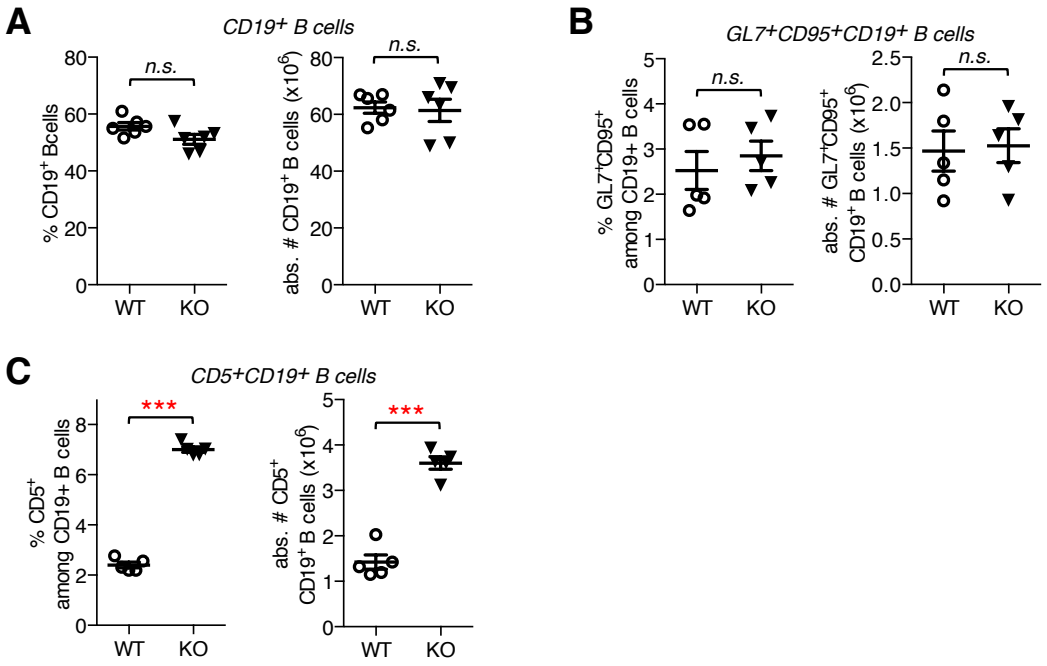

Supplemental Figure 7. Analysis of Toso-deficient B cells during influenza infection.

WT and Toso$^{-/-}$ (KO) mice were infected intranasally with 50 PFU influenza virus strain A/PR8 (H1N1). On day 14 post infection splenocytes were isolated and analyzed by flow cytometry for frequency and numbers of cells that stained positive for the indicated molecules. (**A**) CD19^{+} B cells; (**B**) GL7^{+}CD95^{+} CD19^{+} B cells; (**C**) CD5^{+} CD19^{+} B cells. (**A-C**) Each symbol represents an individual mouse; horizontal line indicates the mean (± SEM). *n*= 5-6; *n.s.,* not significant; ** *P*<0.01; *** *P*<0.001; Students *t* test. Data are representative for at least 3 independent experiments.

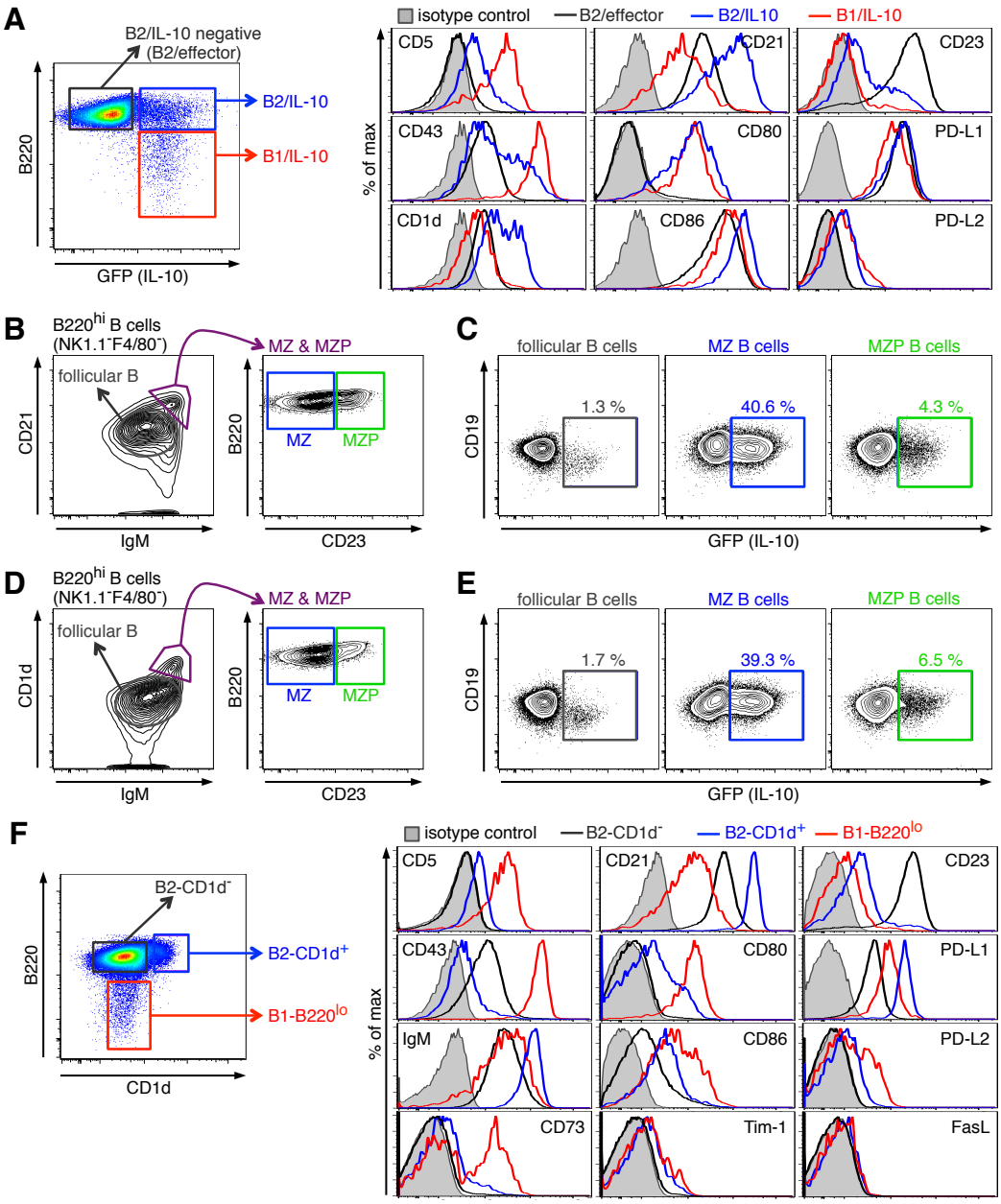

Supplemental Figure 8. Ex vivo characterization of IL-10-producing B cell subsets

(**A**) Purified B cells from IL-10/GFP reporter (Vert-X) mice were treated with BAFF and IL-21 for 16h plus addition of PMA/ionomycin during the last 5 hours. Cells were subsequently stained for the indicated markers and subjected to flow cytometric analysis. Left panel is gated on $CD19^+$ B cells and shows staining for B220 vs GFP to identify B2/effector cells ($B220^{hi}GFP^-$), B2/IL-10 cells ($B220^{hi}GFP^+$) and B1/IL-10 cells ($B220^{lo}GFP^+$). Flow cytometric histograms on the right show expression of the indicated surface markers on B2/effector cells (black line), B2/IL-10 cells (blue line) and B1/IL-10 cells (red line). Gray filled: isotype-matched control. (**B, D**) Gating strategy to isolate follicular, marginal zone (MZ) and marginal zone precursor (MZP) B cells from $B220^{hi}$ B cells that, for higher specificity, were negative for NK1.1 and F4/80. Gating was based on expression of either (**B**) IgM, CD21 and CD23 or (**D**) CD1d, IgM and CD23. (**C, E**) Follicular B cells, MZ B cells and MZP B cells were purified by fluorescence activated cell sorting according to the gating strategy shown on the left in (**B**) or (**D**), respectively. Cells were

stimulated for 16h with LPS plus PMA/ionomycin/BFA/monensin during the last 5 h and subsequently analyzed for IL-10 production. (**F**) Flow cytometric analysis of naïve B cells from C57BL/6J mice. Left panel is gated on $CD19^+$ B cells and shows gating for $B220^{hi}CD1d^-$ cells ('B2-$CD1d^-$'), $B220^{hi}CD1d^+$ cells ('B2-$CD1d^+$') and B1-$B220^{lo}$ cells. Flow cytometric histograms on the right show expression of the indicated surface markers on B2-$CD1d^-$ cells (black line), B2-$CD1d^+$ cells (blue line) and B1-$B220^{lo}$ cells (red line). Gray filled: isotype-matched control. Data are representative for at least 3 independent experiments.

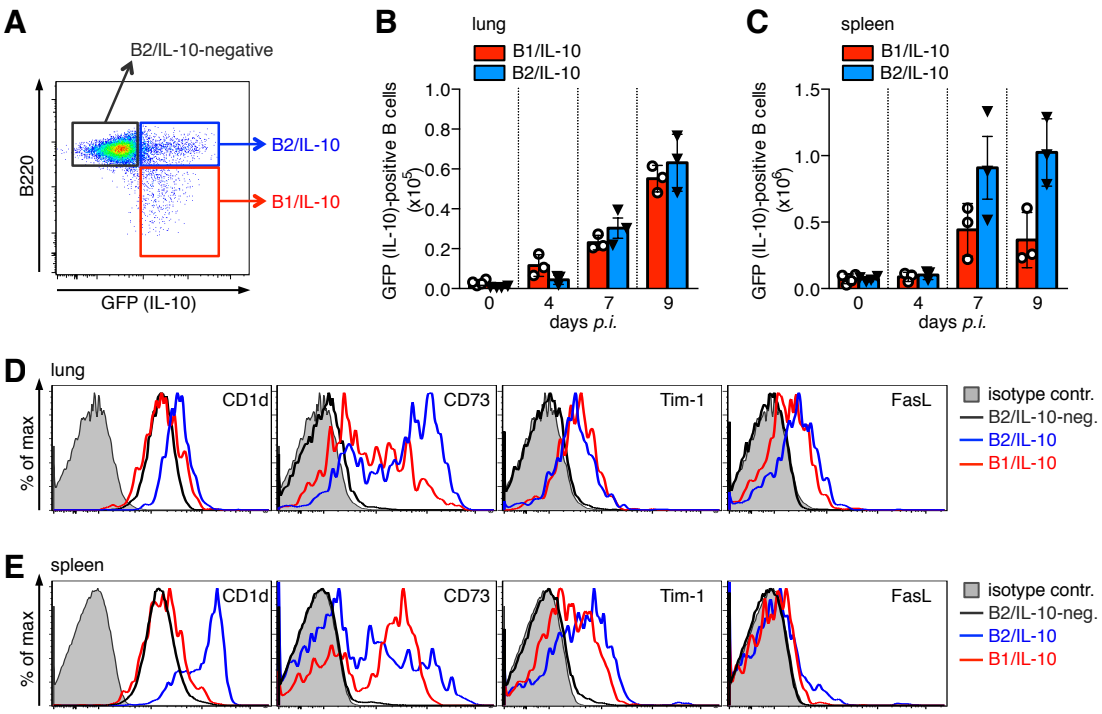

Supplemental Figure 9. Phenotypic analysis of IL-10-producing B cells from influenza A-infected mice

IL-10/GFP reporter (Vert-X) mice were infected intranasally with 1000 PFU influenza virus strain A/PR8 (H1N1). Lung and spleen cells were isolated, treated with PMA/ionomycin for 5 hours and subsequently subjected to flow cytometric analysis. (**A**) Lung cells harvested on day 7 *p.i.* were gated on $CD19^+$ B cells. Panel shows staining for B220 vs GFP to identify B2/IL-10-negative cells ($B220^{hi}GFP^-$), B2/IL-10 cells ($B220^{hi}GFP^+$) and B1/IL-10 cells ($B220^{lo}GFP^+$). (**B, C**) B1/IL-10 cells and B2/IL-10 cells in (**B**) lung and (**C**) spleen from infected animals were quantified at the indicated days *p.i.*. Data are expressed as mean ± SEM; symbols represent individual mice; *n*= 3-4. (**D, E**) Flow cytometric analysis of B cells from (**D**) lung and (**E**) spleen harvested on day 7 *p.i.*. Flow cytometric histograms show expression of the indicated surface markers on B2/IL10-negative cells (black line), B2/IL-10 cells (blue line) and B1/IL-10 cells (red line). Gray filled: isotype-matched control.

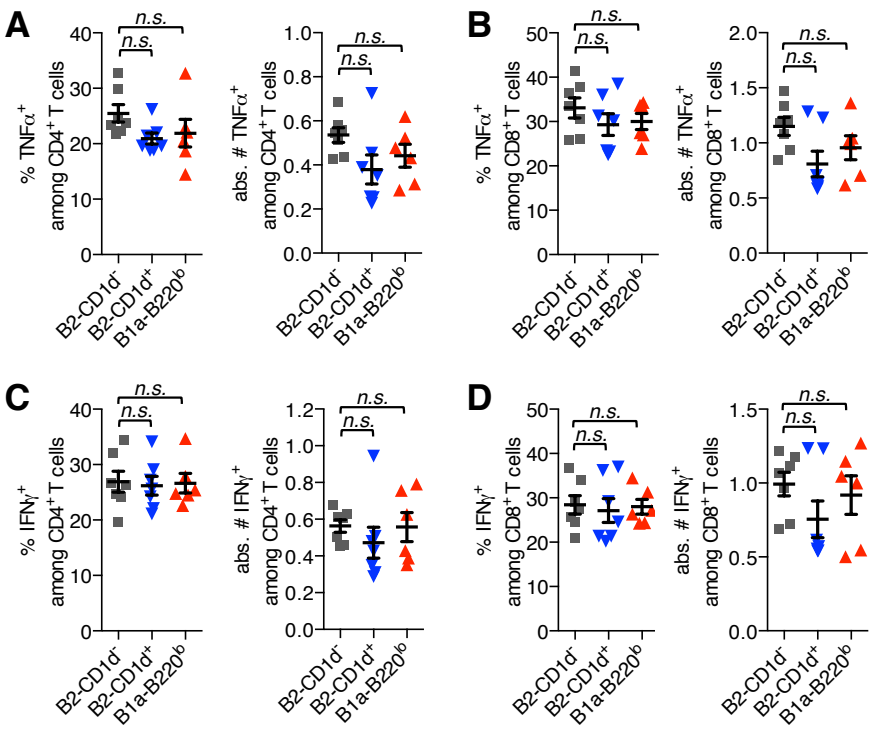

Supplemental Figure 10. Suppressive function of regulatory B cell subsets is dependent on IL-10

$CD19^{+}B220^{hi}CD1d^{-}$ B2 B cells (gray), $CD19^{+}B220^{hi}CD1d^{+}$ B2 B cells (blue) and $CD19^{+}B220^{lo}$ B1a cells (red) were purified from $IL\text{-}10^{-/-}$ (KO) mice by fluorescence activated cell sorting and were adoptively transferred into C57BL/6J mice. Mice were infected intranasally with 1000 PFU influenza virus strain A/PR8 (H1N1). On day 9 *p.i.* lung cells were isolated and analyzed for cytokine staining. Number and frequency of TNFα-producing (**A, B**) and IFNγ-producing (**C, D**) $CD4^{+}$ T cells (**A, C**) and $CD8^{+}$ T cells (**B, D**). Each symbol represents an individual mouse; horizontal line indicates the mean (± SEM). *n*= 6-7; *n.s.*, not significant; one-way ANOVA and Dunnett's post-hoc test. Data are representative for 2 independent experiments.

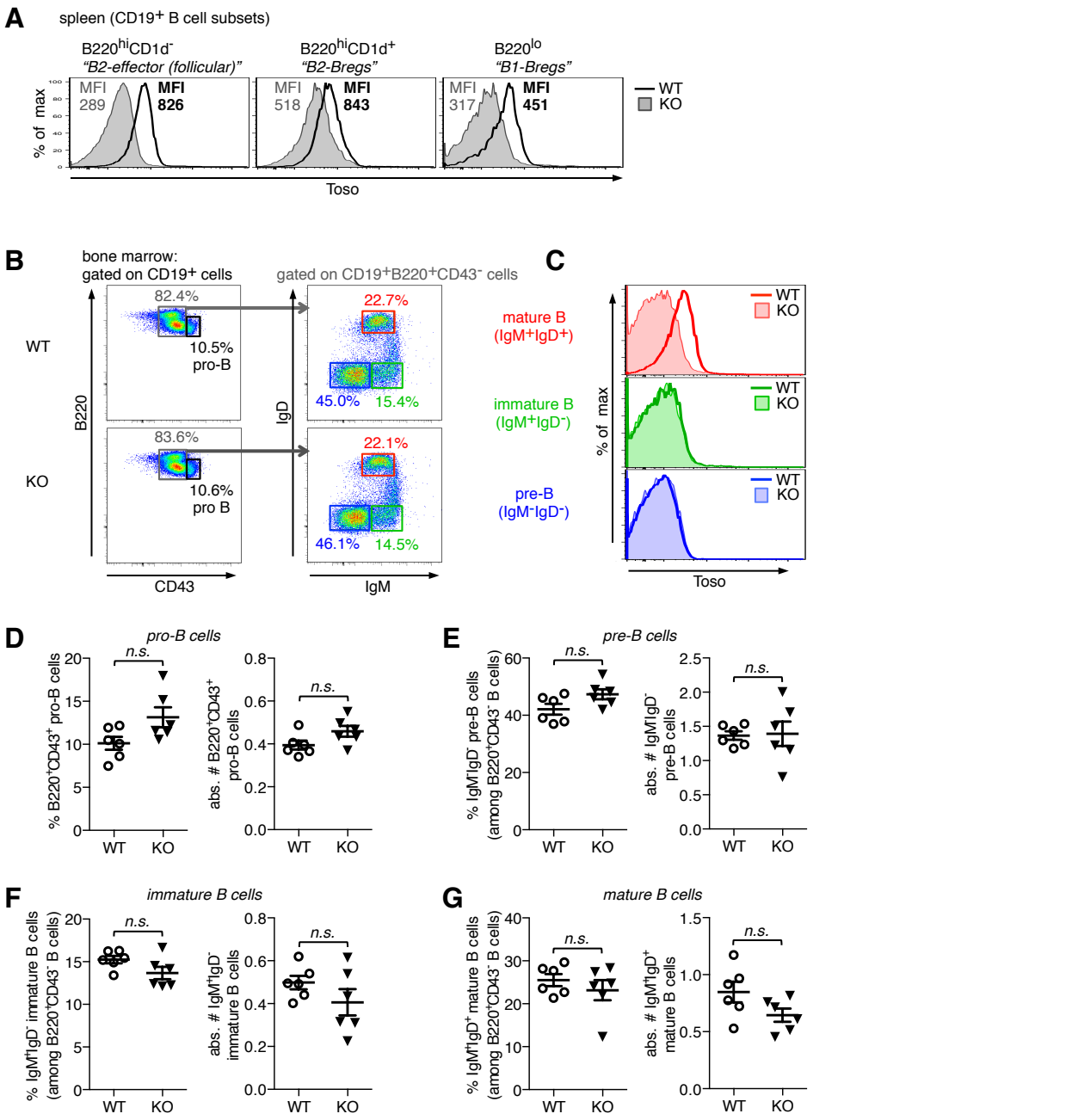

Supplemental Figure 11. Normal B cell development in the bone marrow of Toso-deficient mice.

(**A**) Flow cytometric histograms showing Toso surface expression levels on the indicated $CD19^+$ B cell subsets in the spleen. WT (black line); $Toso^{-/-}$ (KO) (gray filled). GeoMFI, geometric mean fluorescence intensity. (**B-G**) Bone marrow cells from WT and $Toso^{-/-}$ (KO) mice were stained with the indicated surface markers and analyzed by flow cytometry. (**B**) Representative FACS profiles in the left panels are gated on $CD19^+$ cells and show staining for CD43 and B220. Right panels are gated on $CD19^+B220^+CD43^-$ cells and show staining for IgM and IgD. (**C**) Toso surface expression on the indicated B cell subsets in the bone marrow. Cells were pre-gated on $CD19^+B220^+CD43^-$ and Toso expression was analyzed on IgM^+IgD^+ mature B (red), IgM^+IgD^- immature B (green), and IgM^-IgD^- pre-B cells (blue). (**D-G**) Frequency and absolute number of

the indicated B cell subpopulations in the bone marrow of WT and Toso$^{-/-}$ (KO) mice. Analysis was performed on CD19^{+} cells (**D**) and CD19^{+}B220^{+}CD43^{-} cells (**E-G**). Data show B220^{+}CD43^{+} pro-B cells (**D**), IgM^{-}IgD^{-} pre-B cells (**E**), IgM^{+}IgD^{-} immature B cells (**F**), and IgM^{+}IgD^{+} mature B cells (**G**). (**D-G**) Each symbol represents an individual mouse; horizontal line indicates the mean (± SEM); *n*=6; *n.s.,* not significant; Students *t* test. Data are representative for at least 3 independent experiments.

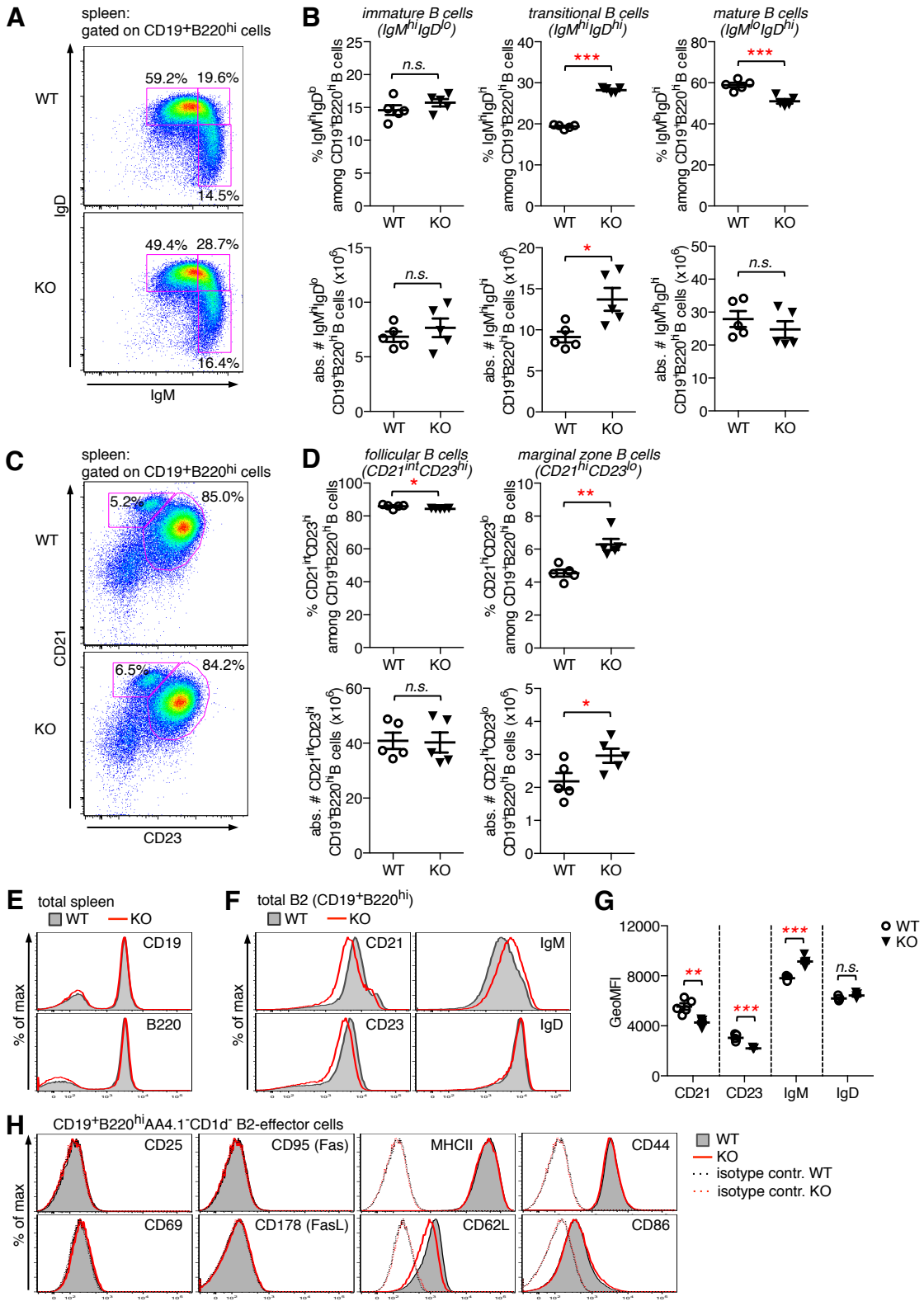

Supplemental Figure 12. Altered development and maturation of splenic B cells in Toso-deficient mice.

Splenocytes from WT and Toso$^{-/-}$ (KO) mice were stained with the indicated surface markers and analyzed by flow cytometry. (**A**) Representative FACS profiles are gated on CD19^{+}B220^{hi} cells

and show staining for IgM and IgD. (**B**) $CD19^{+}B220^{+}$ B cells were analyzed for frequency and absolute number of $IgM^{hi}IgD^{lo}$ immature B cells, $IgM^{hi}IgD^{hi}$ transitional B cells, and $IgM^{lo}IgD^{hi}$ mature B cells. (**C**) FACS profiles are gated on $CD19^{+}B220^{hi}$ cells and show staining for CD23 and CD21. (**D**) $CD19^{+}B220^{+}$ B cells were analyzed for frequency and absolute number of $CD21^{int}CD23^{hi}$ follicular B cells and $CD21^{hi}CD23^{lo}$ marginal zone B cells. (**B, D**) n=5. (**E**) CD19 and B220 surface levels on spleen cells from WT (gray filled) and $Toso^{-/-}$ (KO) mice (red line). (**F, G**) Surface expression levels of CD21, CD23, IgM and IgD on $CD19^{+}B220^{hi}$ B2 cells from WT and $Toso^{-/-}$ (KO) mice. (**F**) Representative flow cytometric histograms and (**G**) geometric mean fluorescence intensity (GeoMFI; n=5) ± SEM are shown. (**H**) Flow cytometric histograms showing representative surface expression levels of the indicated surface receptors on $B220^{+}AA4.1^{-}CD1d^{-}$ B2-effector cells from WT (gray filled) and $Toso^{-/-}$ (KO) mice (red line). Dotted lines show isotype-matched control stainings. Data are representative for at least 3 independent experiments. * P<0.05; ** P<0.01; *** P<0.001; Students t test.

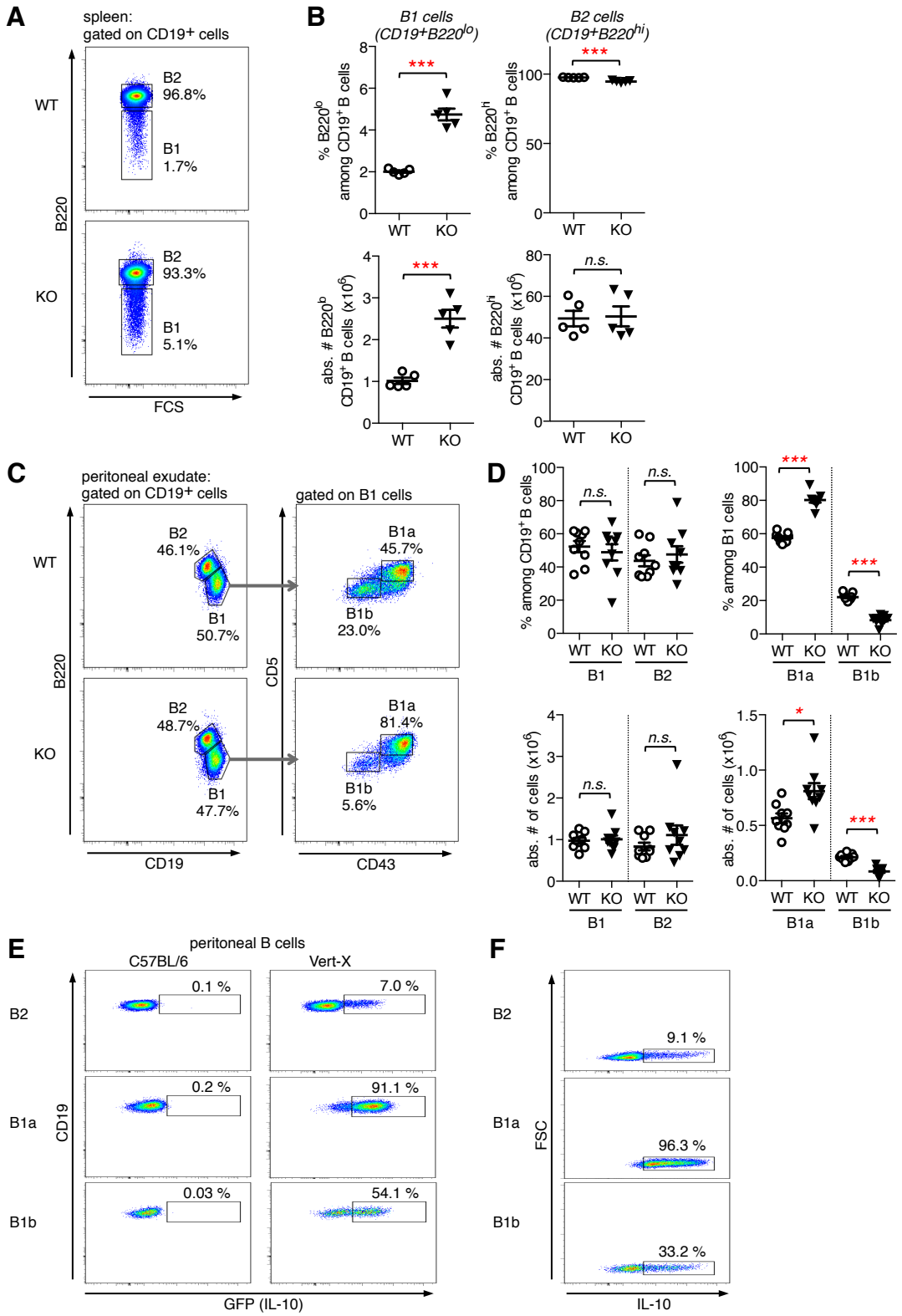

Supplemental Figure 13. Splenic and peritoneal B1a B cells are increased in Toso-deficient mice.

(**A, B**) Flow cytometric analysis of splenocytes from WT and Toso$^{-/-}$ (KO) mice. (**A**) FACS profiles are gated on CD19+ cells and show staining for FSC vs. B220. (**B**) Frequency and

number of $CD19^{+}B220^{lo}$ B1 B cells and $CD19^{+}B220^{hi}$ B2 B cells in the spleen of WT and $Toso^{-/-}$ (KO) mice. (**C, D**) Peritoneal exudate cells from WT and $Toso^{-/-}$ (KO) mice were stained with the indicated surface markers and analyzed by flow cytometry. (**C**) Left panel: FACS profiles are gated on $CD19^{+}$ cells and show staining for CD19 and B220. Gating for B1 and B2 cells is indicated. Right panel: FACS profiles are gated on B1 cells and show staining for CD43 and CD5. Gating for B1a and B1b cells is indicated. (**D**) Frequency and number of B1 and B2 cells (left panel), and B1a and B1b cells (right panel) in the peritoneal exudate from WT and $Toso^{-/-}$ (KO) mice. Each symbol represents an individual mouse; horizontal line indicates the mean (± SEM). *n.s.,* not significant; * $P<0.05$; ** $P<0.01$; *** $P<0.001$; Students *t* test. (**E**) Peritoneal exudate cells from IL-10/GFP reporter Vert-X mice (right panel) were treated for 5h with LPS and PMA/ionomycin. Cells were stained for CD19, B220, CD5 and CD43 and analyzed by flow cytometry. B2, B1a and B1b subpopulations were identified as shown in (C) and analyzed for GFP expression as a marker for IL-10 production. Cells from normal C57BL/6 mice were treated similarly and served as a negative control (left panel). (**F**) Peritoneal exudate cells form normal WT C57BL/6 mice were treated for 5h with LPS and PMA/ionomycin in the presence of brefeldin A. IL-10 production in B2, B1a and B1b cells was subsequently analyzed by intracellular cytokine staining. (**B, D**) Each symbol represents an individual mouse; horizontal line indicates the mean (± SEM). (**B**) $n=5$; (**D**) $n=9$. *n.s.,* not significant; * $P<0.05$; ** $P<0.01$; *** $P<0.001$; Students *t* test. Data are representative for at least 3 independent experiments.

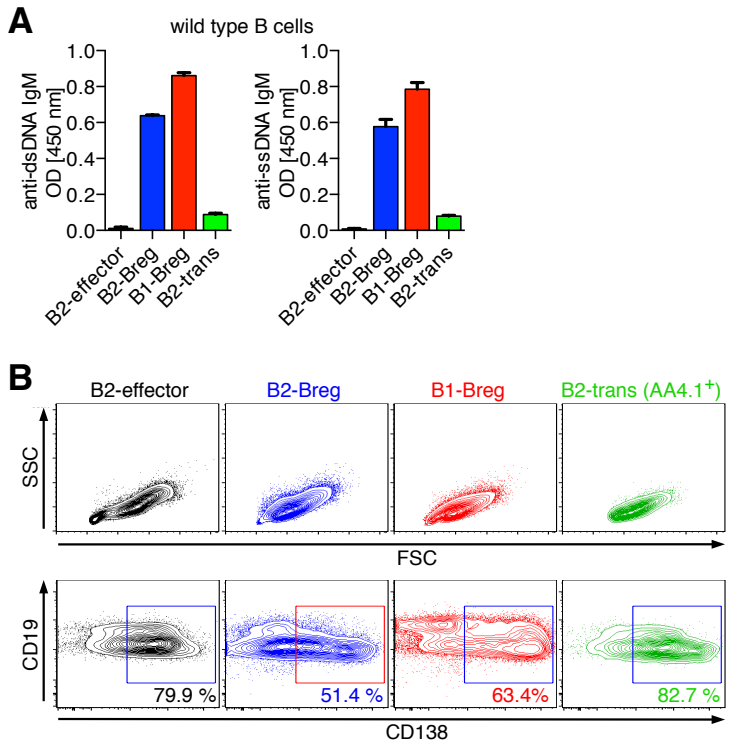

Supplemental Figure 14. Self-reactivity of IL-10-competent regulatory B cell subsets.

$B220^{hi}AA4.1^{-}CD1d^{-}$ B2-effector cells, $B220^{hi}CD1d^{+}$ B2-Bregs, $B220^{hi}AA4.1^{+}$ B2-transitional cells (B2-trans) and $B220^{lo}$ B1-Bregs from WT mice were purified by flow cytometric cell sorting and were treated for 3 days with LPS. (**A**) Culture supernatants were analyzed for anti-dsDNA and anti-ssDNA IgM levels (n=2). (**B**) Cells were analyzed by flow cytometry for forward scatter (FSC) vs side scatter (SSC) characteristics and CD138 vs CD19 surface expression. Data are representative for at least 2 independent experiments.

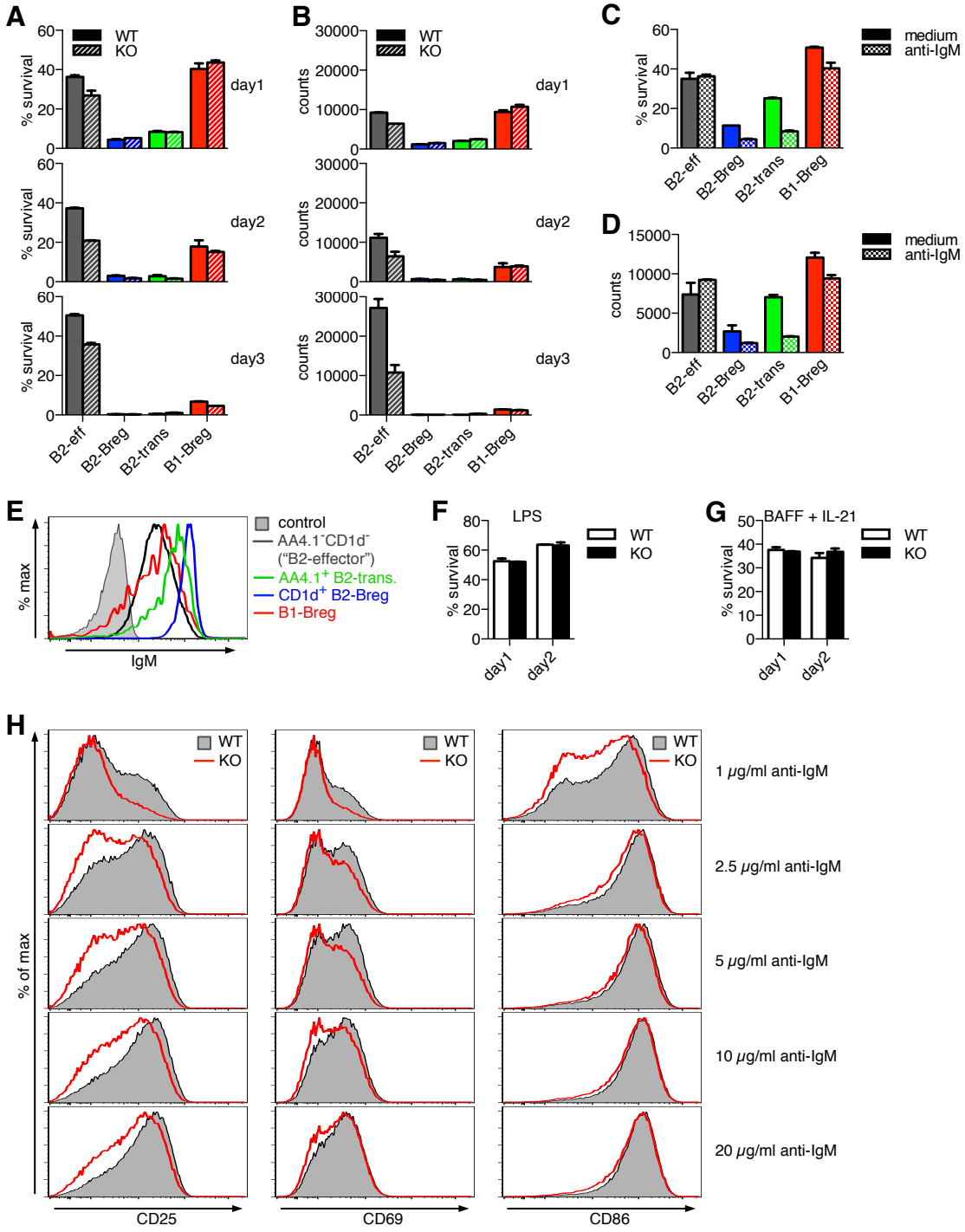

Supplemental Figure 15. Altered BCR-responsiveness of Toso-deficient B2-effector B cells.

(**A-D**) AA4.1$^-$CD1d$^-$ B2-effector cells, AA4.1$^+$ B2-transitional cells, CD1d$^+$ B2-Bregs and B220^{lo} B1-Bregs were purified by flow cytometric cell sorting. (**A-B**) High purity sorted B cell subsets from WT (filled bars) and Toso$^{-/-}$ (KO) (hatched bars) mice were stimulated for the indicated times with anti-IgM and analyzed by flow cytometry for (**A**) cell survival and (**B**) cell counts. (**C, D**) High-purity sorted B cell subpopulations from C57BL/6 mice were either cultured with medium (filled bars) or were stimulated with anti-IgM (15 μg/ml; patterned bars). After 24 h cultures were analyzed by flow cytometry for (**C**) cell survival and (**D**) proliferation (cell counts).

Data show results for $B220^{hi}AA4.1^{-}CD1d^{-}$ B2-effector cells (dark gray), $B220^{hi}CD1d^{+}$ B2-Bregs (blue), $B220^{hi}AA4^{+}$ B2-transitional cells (green) and $B220^{lo}$ B1-Bregs (red). Data are mean ± SEM from two independent cultures. (**E**) IgM surface expression levels on naïve (=unstimulated) B cell subsets. (**F, G**) Purified $CD19^{+}$ B cells from WT and $Toso^{-/-}$ (KO) mice were treated with (**F**) LPS or (**G**) BAFF plus IL-21. At the indicated times, cultures were analyzed by flow cytometry for cell survival. Data are mean ± SEM from 2 independent cultures. (**H**) Sorted B2-effector cells were stimulated for 16h with titrated concentrations of anti-IgM and analyzed by flow cytometry for upregulation of the B cell activation markers CD25, CD69 and CD86. WT (gray filled); $Toso^{-/-}$ (KO) (red line). Data are representative for at least 3 independent experiments.

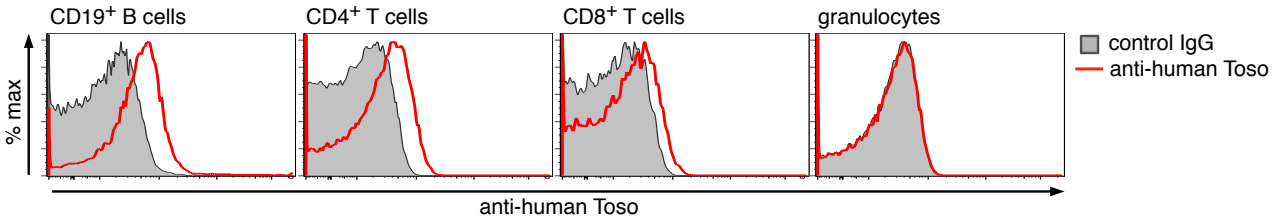

Supplemental Figure 16. Toso-expression on human lymphocytes

Flow cytometric analysis of human peripheral blood cells showing surface expression of human Toso on $CD19^+$ B cells, $CD4^+$ T cells, $CD8^+$ T cells and granulocytes. Staining with control IgG (gray filled); anti-human-Toso mAb staining (red line). Anti-human-Toso mAb recognizing the extracellular portion of human Toso was generated by utilizing DNA-immunization of rats. Data are representative for at least 2 independent experiments.

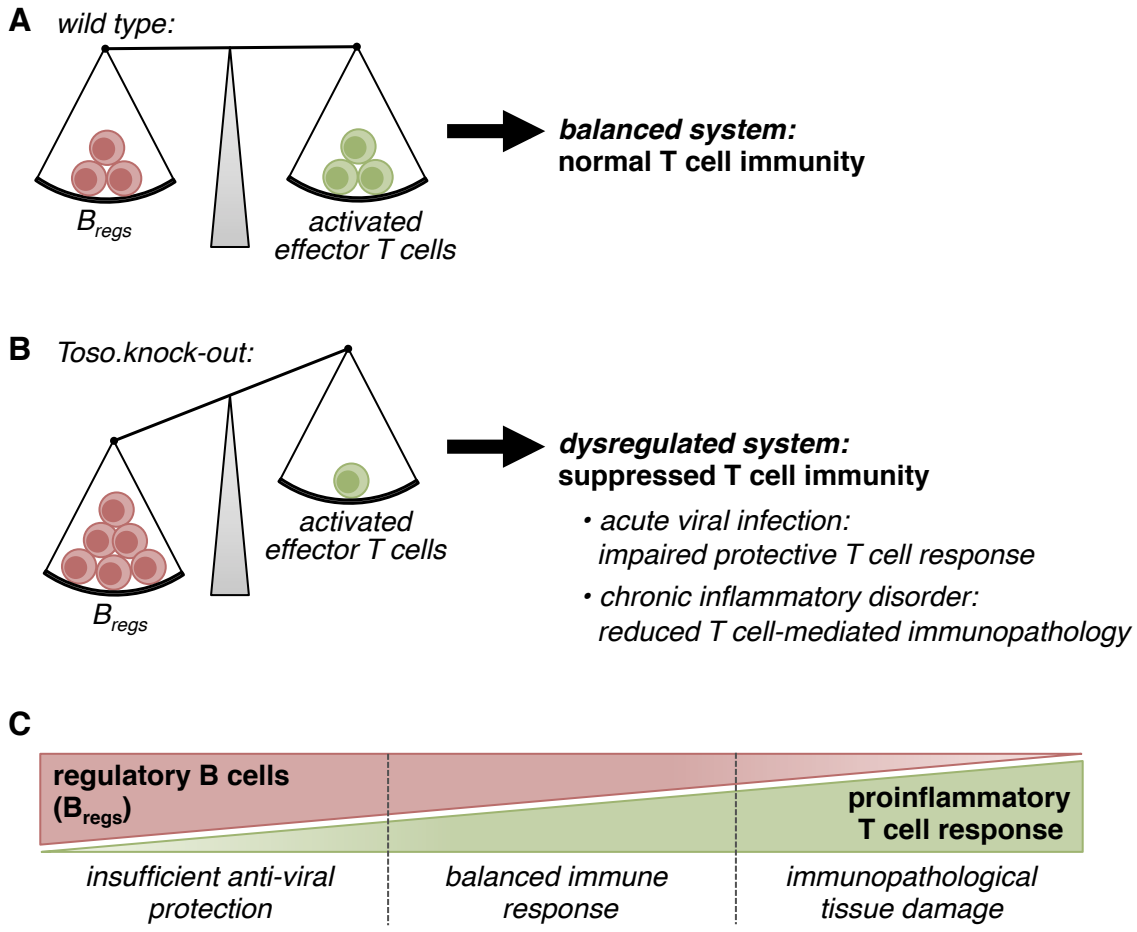

Supplemental Figure 17. Model: Effects of Toso-deficiency on regulatory B cells and T cell immune responses: implications for protective immunity vs immunopathology

Based on our data we propose the following model to explain the immune defects observed in Toso-deficient mice. (**A**) In normal wild type mice the ratio of regulatory B cells (B_{regs}) to effector T cells is tightly balanced, allowing for normal protective T cell immunity. (**B**) Toso-deficiency on B cells leads to increased numbers of B_{regs} that exhibit immunosuppressive activity on effector T cells, resulting in reduced proinflammatory T cell responses. Depending on the type of inflammatory disease and the particular role of T cells in this disease, such suppressed T cell immunity can have different consequences: During acute viral infection (e.g. acute influenza infection), where anti-viral immunity is largely T cell-dependent, impaired T cell responses are detrimental and result in insufficient pathogen clearance and thus defective immune protection. On the other hand, during chronic inflammatory disorders (e.g. chronic *Salmonella*-induced intestinal inflammation), where T cell effector function is more associated with immunopathological tissue damage, higher numbers of B_{regs} and thus reduced T cell effector function is beneficial, as this limits the extend of T cell-mediated tissue destruction. (**C**) High numbers of immunosuppressive B_{regs} (such as e.g. in Toso-deficient mice) are associated with impaired proinflammatory T cell responses and, thus, insufficient anti-viral activity, but provide relative protection from T cell-mediated tissue damage. Conversely, low numbers of B_{regs} are associated with strong proinflammatory T cell responses that provide efficient immune protection against invading pathogens, but on the downside, may also cause immunopathological tissue

destruction. In a normal healthy system, B_{reg} numbers are well balanced, thus allowing for pathogen clearance by T cells, while avoiding excessive T cell activation, thus limiting immunopathological tissue damage.